The Thesis Committee for Tianyi Cheng

Certifies that this is the approved version of the following thesis:

Solar Ultraviolet Irradiation Activates IFNγ/STAT1 Signaling Pathway in the Epidermis

APPROVED BY

SUPERVISING COMMITTEE:

_____

John DiGiovanni, Supervisor

_____

Edward Mills

Solar Ultraviolet Irradiation Activates IFNγ/STAT1 Signaling Pathway in the Epidermis

By

Tianyi Cheng, B.E.

Thesis

Presented to the Faculty of the Graduate School

of the University of Texas at Austin

in Partial Fulfillment

of the Requirements

for the Degree of

Master of Science in Pharmaceutical Sciences

The University of Texas at Austin

December 2015

Dedication

This dissertation is lovingly dedicated to my family.

Acknowledgements

Graduate study provides me not only the means to understand problems and discover mechanism but also the opportunity to identify personal potential and increased self-awareness. My mentor, Dr. John DiGiovanni gave me this precious chance. I am indebted to his efforts to train me in science as an independent researcher with the ability to think in depth and his willingness to enrich me with this life experience. Especially, I appreciate his personal side for his understanding, insightful advice and full support in the pursuit of my career path, and also for tolerating my immaturity and sharing his stories and life experiences during graduate school. The aid from other faculties in College of Pharmacy should not be neglected and they together made this thesis possible.

To my lab colleagues, and at the same time my dearest friends, I would like to cordially thank them for help and encouragement throughout the past years. They have helped me on the bench top, and this professional and friendly atmosphere has made my research hours both fruitful and enjoyable. Steve Carbajal and Dr. Jaya Srivastava have always been willing to discuss with me on, but not limited to, my project and help come up with insightful suggestions. Past lab members including Dr. Ronald Bozeman and Dr. Everado Macias provided me with invaluable mentorship early on in my academic path. My current and past lab colleagues all gladly helped me improve my communication skills and they will always, or at least pretend to, laugh at my English jokes. I wish them all the best.

Finally, I acknowledge with gratitude, the support and love of my family in China; my cousin, Ranran Zhang and my girlfriend, Yun Shang, in the US. My achievement would be unimaginable without them.

My work was not fulfilled in a day; instead, it was built by each and every piece of help from my teachers, friends and colleagues during the past three years. For those whose names are not listed, I want to express my heartfelt appreciation. You

all keep me going. I was happy about taking this academic sojourn with all of you.

Solar Ultraviolet Irradiation Activates IFNγ/STAT1 Signaling Pathway in the Epidermis

By

Tianyi Cheng, M.S.P.S.

The University of Texas at Austin, 2015

SUPERVISOR: John DiGiovanni,

Signal transducer and activator of transcription 1 (STAT1) is a latent transcription factor activated by Interferon gamma (IFNγ) receptor. The role of STAT1 in epithelial carcinogenesis remains poorly defined. Previous work performed in our lab showed that STAT1 was absolutely required for skin cancer promotion by chrysarobin using the multistage skin carcinogenesis model. A novel mechanism of skin tumor promotion involving IFNγ/STAT1 signaling was defined. Interestingly, Solar ultraviolet (SUV) radiation activated IFNγ/STAT1 pathway in a similar pattern as seen with chrysarobin. SUV treatment led to rapid phosphorylation of STAT1 on both tyrosine (Y701) and serine (S727) residues in epidermis. An increase of unphosphorylated STAT1 (uSTAT1) and interferon regulatory factor 1 (IRF1) were also observed and verified to be dependent on STAT1 activation. Further analyses demonstrated that the induction of phosphorylation of STAT1, and the increase of both IRF1 and uSTAT1 was dependent on intact IFNγ signaling. Quantitative PCR detected an increase of STAT1, IRF1 and other downstream targets of IFNγ/STAT1 axis including Cxcl9, Cxcl10, Cxcl11, PD-L1 and Cox2, which all depended on STAT1 activation. IFNγ receptor knockout mice displayed no activation of the IFNγ/STAT1 signaling

pathway, weak activation of MAPK signaling and reduced myeloid cells influx into the dermis following exposure to SUV. CD3+ cells were determined to be the only source of IFNγ production in the epidermis following SUV treatment. Also, CD3+ cells were the primary cellular source of IFNγ production after CHRY treatment. A topical ointment application containing an oligonucleotide decoy was formulated to inhibit the activation of IFNγ signaling in the epidermis. Collectively, these findings clearly demonstrate that SUV activates the IFNγ/STAT1 signaling pathway in the mouse epidermis.

Tables of Contents

List of Illustrations

Chapter 1

Chapter 3

Chapter 4

Chapter 5

Chapter 6

Chapter 7

Chapter 8

Chapter 1: Introduction

1.1 Signal Transducers and Activators of Transcription

Signal Transducers and Activators of Transcription (STATs) are a family of latent cytoplasmic transcription factors that transduce extracellular signals from the cell membrane to the nucleus [1]. Consisting of STAT1, Stat2, STAT3, STAT4, STAT5A/B and STAT6, STATs are involved in many different physiological regulatory events, including hematopoiesis, immunomodulation and development [2, 3]. On the other hand, aberrant Stat signaling has been associated with various pathological events, including oncogenesis. Of all the Stat family members, STAT1, STAT3 and STAT5 are found frequently to be constitutively activated in human tumors [4, 5]. STATs are activated by a variety of factors such as cytokines, growth factors, hormones and oncogenic signals. Following the binding of cytokines to their cognate receptors, STATs are activated by members of the janus activated kinase (JAK) family of tyrosine kinases. Once activated, they dimerize and translocate to the nucleus and modulate the expression of target genes (Fig. 1.1) [6-8]. JAK/STAT signaling is mechanistically simple with only a few principal components to translate an extracellular signal into transcriptional responses [9, 10].

STATs exhibit a modular structure with six well-defined domains, including an N-terminal-conserved domain, a coiled-coil domain, a DNA binding domain, a linker region, an SH2 domain and a C-terminal transactivation domain (Fig 1.2). The SH2 domain, which is highly conserved among the STATs, plays a very important role in STAT signaling being critical for the recruitment of STATs to activated receptor complexes and for the interaction with JAK and Src kinases. Cytokine stimulation induces phosphorylation of tyrosine residues on the receptor that serve as docking sites for STATs via their SH2 domains. Once bound to the

receptor, all members of the STAT family become tyrosine phosphorylated in response to cytokine stimulation at a conserved C-terminal tyrosine, (e.g. Y701 for STAT1, Y705 for STAT3). Phosphorylation of this tyrosine appears to be achieved by growth factor receptors as well as by JAK and Src kinases, depending on the nature of the cell type and the ligand/receptor interactions. This form of phosphorylation induces STAT homodimerization and heterodimerization via the interaction of the phosphotyrosine residue of one STAT molecule with the SH2 domain of another. The dimers then translocate into the nucleus by binding to importin-α and then induce target gene expression [11].

In addition to this canonical view of STAT signaling, it has now been firmly established that many if not all STAT proteins can exist as preformed dimers, which are unable to bind DNA, in the absence of the activating tyrosine phosphorylation [12]. However, the molecular interfaces that drive dimerization differ between individual STATs. The interaction of N-terminal domain has been found to be necessary for the dimerization of nonphosphorylated STATs [13].

Previous investigations of Stat1 protein have identified three STAT1 protein forms: monomer, antiparallel unphosphorylated dimer and reciprocal pY-SH2 parallel phosphorylated dimer (Fig 1.3). During the activation-inactivation cycle, STAT1 goes through conformational rearrangement from parallel to antiparallel structure [14-16]. The crystal structure for tyrosine phosphorylated STAT1 dimer bound to DNA has been determined [17]. The structure verified that the SH2 domain necessary for dimerization is also involved in DNA binding. Moreover, some kinases can phosphorylate STAT1 at serine 727 (S727). This phosphorylation can occur independently of tyrosine phosphorylation and is not required for STAT1 translocation to the nucleus or for its binding to target gene promoters. However, it is essential for the full transcriptional activation [18].

In previous work performed in our laboratory, we established a critical role for

STAT3 in both chemical- and UVB-mediated epithelial carcinogenesis [19]. In a chemical-mediated epithelial carcinogenesis model, STAT3 was shown to be important during the initiation phase of epithelial carcinogenesis by regulating keratinocyte survival, including survival of bulge-region keratinocyte stem cells [20, 21]. STAT3 was also shown to be important for the clonal expansion of initiated cells during tumor promotion by regulating key cell cycle progression proteins such as cyclin D1 and c-myc [20, 22]. Furthermore, STAT3 was found to also play a significant role in the progression of skin tumors via its ability to regulate genes involved in angiogenesis and epithelial-mesenchymal transition [23]. Furthermore, STAT3 was shown to play an important and similar role in UVB-mediated skin carcinogenesis [24, 25]. However, the exact role of other STATs in multistage epithelial carcinogenesis remains largely unknown at present.

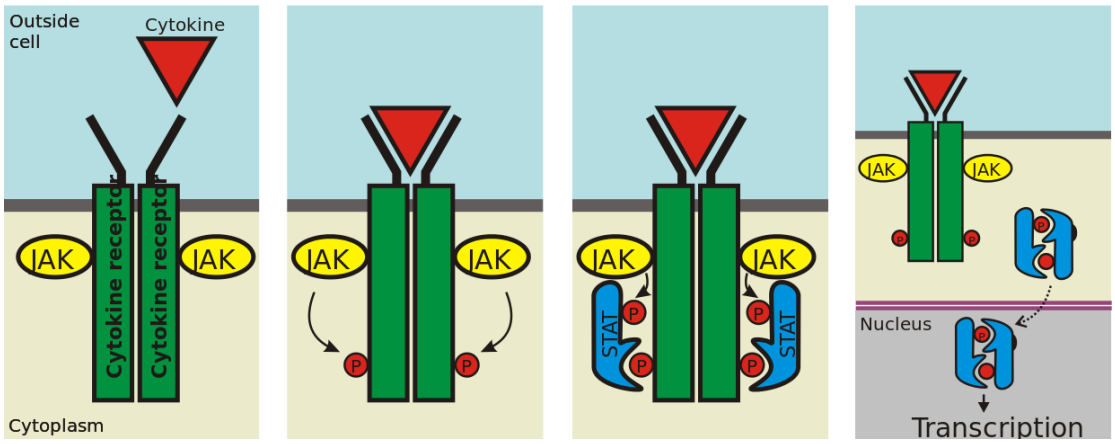

Figure 1.1 Key Steps of the JAK-STAT pathway

Upon cytokine ligand binding to the cell surface receptors, JAK kinases phosphorylate the receptors, generating docking sites for the normally cytosolic STATs. After phosphorylated by JAK kinases, STATs dimerize and translocate to the nucleus and bind to the promoters of target genes to activate their transcription. From Peter Znamenkiy (2008)

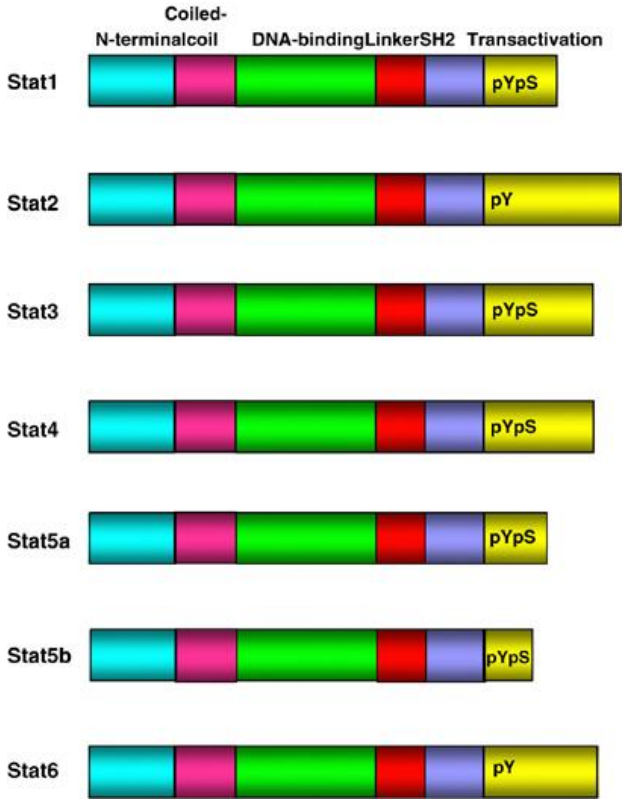

Figure 1.2 Structure of STAT proteins

STATs harbor six domains, the N-terminal, coiled-coil, DNA-binding, linker, SH2 and transactivation domains. The N-terminal and DNA binding domains cooperate in binding to the promoters of target genes.

Regulatory phosphotyrosine (pY) and phosphoserine residues (pS) are also shown [26].

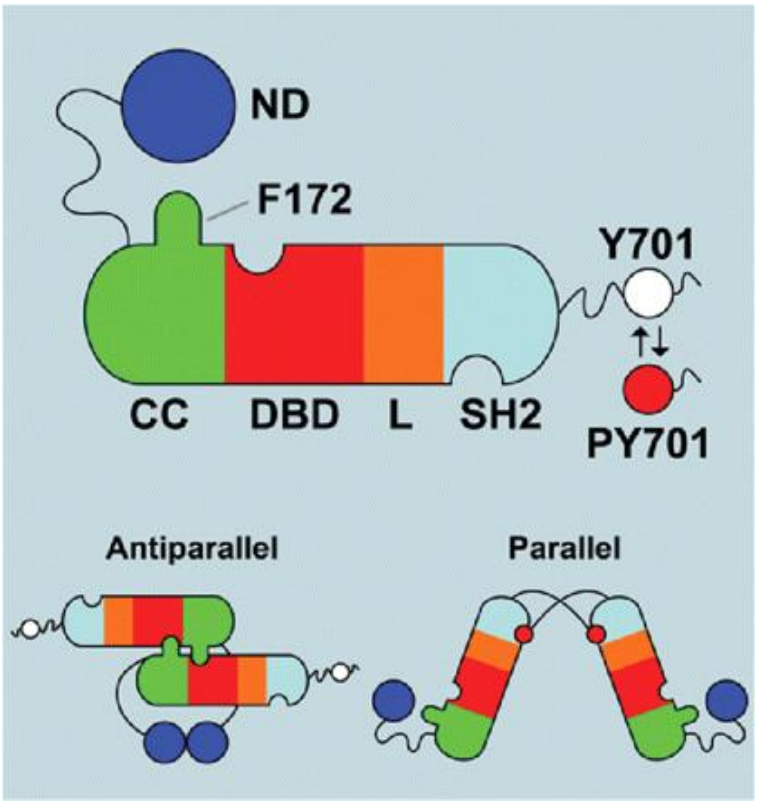

Figure 1.3 Schematic of notable features of STAT1 protein structure
The domains are N-terminal domain (ND), coiled:coil domain (CC), DNA-binding domain (DBD), linker domain (L), and SH2 domain (SH2). The ND is shown tethered to the CC through a flexible linker, and the residues C-terminal to –SH2 include Y701, which is phosphorylated (red) when the molecule is activated. The C-terminal region is also flexible as indicated by the wavy black line. At the bottom of the figure are diagrams of the parallel and antiparallel structures. Notable is the F172 residue that is important in the antiparallel structure [16].

1.2 Two Stage Carcinogenesis Model

The classic two-stage, initiation-promotion model of skin carcinogenesis is a chemically-induced model of epithelial carcinogenesis that enables evaluation of three stages of tumor development, including tumor initiation, promotion and progression [27]. In standard protocols, topical application of a single subcarcinogenic dose of a carcinogen (e.g. 7,12-dimethylbenz(a)anthracene [DMBA]) induces irreversible DNA mutations in critical genes, including H-ras and K-ras, in keratinocyte stem cells in the bulge region of the hair follicles. Repeated topical treatment of a non-carcinogenic promoting agent, such as TPA or CHRY, can induce epidermal hyperplasia and cell proliferation. The initialed stem cells, during repetitive exposure to a promoting stimuli, have a selective growth advantage such that these cells undergo clonal expansion. The endpoint of the promotion stage in the mouse skin model is the formation of squamous papillomas, which are exophytic, noninvasive lesions consisting of hyperplastic epidermis folded over a core of stroma. The process of tumor progression occurs when papillomas convert to skin cell carcinomas (SCC). The SCCs that develop in this model are histologically very similar to human SCCs of the skin [reviewed in Epithelial Skin Cancer, *The Molecular Basis of Cancer*, 2015]. This model has been well characterized and bears relevance to human epithelial cancers, thereby providing an excellent paradigm for the study of mechanisms associated with multistage epithelial carcinogenesis (Fig. 1.4) [28].

Tumor promoting stimuli are very diverse in this model and include various chemicals such as phorbol esters (e.g. TPA), organic peroxides (e.g. benzoyl peroxide), anthrones (e.g. CHRY) and so on. Additionally, UV light, repeated abrasion, full thickness skin wounding, and certain silica fibers when rubbed on the skin all function as skin tumor promoting stimuli. Most tumor promoters are not

genotoxic but cause altered expression of genes whose products are associated with hyperproliferation, tissue remodeling, and inflammation. A number of changes in growth regulatory proteins and molecules occur during tumor promotion in the mouse skin model and are thought to stimulate a cascade of cell signaling events that alter cell proliferation and/or differentiation. The exact mechanisms for the way in which the different types of tumor promoters bring about the cellular, biochemical and molecular changes associated with the process of skin tumor promotion remains to be fully elucidated. For the phorbol ester type tumor promoters, the cellular receptor that initiates their actions is protein kinase C [29]. For compounds that break down to form reactive oxygen species (ROS) and other types of radical intermediates such as the anthrones (e.g. CHRY) and the organic peroxides (e.g. benzoyl peroxide), it is believed that they work by inducing oxidative stress that activates multiple signaling pathways associated with skin tumor promotion [30, 31].

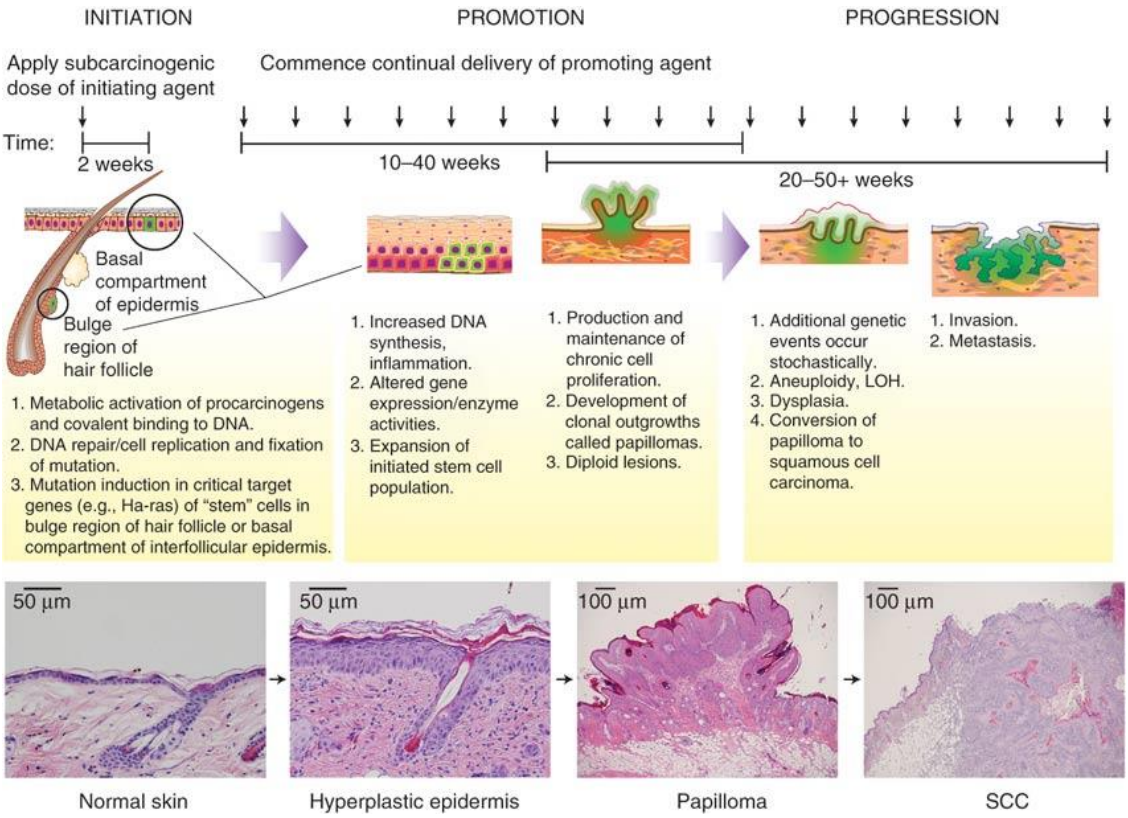

Figure 1.4 Two-stage model of skin carcinogenesis in mice

During initiation, topical application of a sub-carcinogenic dose of a mutagenic agent induces mutations in target genes in keratinocyte stem cells. Repeated topical application of a promoting agent begins 2 weeks after initiation and continues for the duration of the study. Papillomas begin to arise after ~6–12 weeks of promotion and a fraction begin to convert to SCC after ~20 weeks. Representative H&E stained sections of normal skin, hyperplastic skin, a papilloma and a SCC are presented [28].

1.3 Ultraviolet Radiation and Non-Melanoma Skin Cancer

Wavelengths of both ultraviolet A (UVA 320-400 nm) and ultraviolet B (UVB 280-320 nm) radiation have been implicated as carcinogens, though their methods of action are not the identical. The two wavelengths of radiation are able to penetrate to different depths of the skin and hence affect different cells in the epidermis and dermis: UVB radiation is mainly absorbed by epidermal components such as proteins or deoxyribonucleic acid (DNA), whereas UVA radiation penetrates deeply into the skin and reaches the lower epidermis and dermal fibroblasts. Other than tumorigenic predilection, UV radiation also disrupts keratinocytes in the skin epithelia, causing other immunological and inflammatory disorders [32].

The extent of their effect also varies, with UVB being described as the most carcinogenic among all types of solar radiation. UVB radiation's main deleterious effect is DNA damage caused by its direct interaction with the molecule, while UVA radiation's toxicity mainly comes from oxidative damage to skin cell components including DNA damage [33].

Nonmelanoma skin cancer is the most common cancer and consists of basal cell carcinoma and squamous cell carcinoma (SCC). Every year in the US, the incidence of nonmelanoma skin cancer excelled three million, leading to a significant economic burden for the society. Excessive exposure to sunlight radiation has been well documented to be the major cause of nonmelanoma skin cancer [34]. Because of its public health relevance and the need to understand the biologic impact of UV irradiation on the skin, there has been a long-standing interest in the mechanisms by which this form of radiant energy causes skin cancer. Observations from this line of investigation have led to a better understanding of UV-induced skin cancer specifically and, more broadly, of cancer in general.

The UVB range is generally found to be most effective in inducing skin cancer and most studies in the literature were conducted using lamps emitting mostly UVB. The signal transduction pathway and key molecules involved in the solar ultraviolet (SUV) -induced skin disorders including tumorigenesis are not yet completely elucidated. However, it has been clearly shown that UVA (320-400 nm) and UVB (280-320 nm) both function as initiators and promoters in carcinogenesis and possess immunosuppressive activity [35](thoroughly reviewed in IARC Monographs Vol55 and Vol100D). Moreover, on the surface of the Earth, UVA wavelengths are the most abundant (over 95%) in the sunlight UV spectrum. Therefore, the role of UVA wavelengths in skin tumorigenesis due to chronic sun exposure is worthy of further investigation (Fig. 1.6).

A comparison of commercial SUV and UVB lamps are illustrated (Fig. 1.5). The UVB lamp emits a significant amount of UV in wavelengths shorter than 295 nm. These wavelengths are not found in sunlight, and for carcinogenesis induction, the UVB lamp can be unrealistically effective. To eliminate any unnatural results from the short-wavelength UV, the work in this thesis was performed using a light source generating both UVA and UVB by the ratio over 15:1 to mimic the UV emission of the sun (Ball, James C. 1995. A comparison of the UV-B irradiance of low-intensity, full-spectrum lamps with natural sunlight. Bulletin of the Chicago Herpetological Society. 30 (4):69-72.). This lamp was utilized by other researchers with success [36].

A number of contributing mechanisms to UV-induced skin tumorigenesis have been defined [37, 38]. For example, multiple signaling pathways may be activated in response to UVB including PKC, AhR, EGFR/ErbB, IL12, AP-1 and Cox-2 [29, 39]. UVA wavelengths, which penetrate deeply into the skin, induce formation of ROS and oxidative stress in both epidermal keratinocytes and dermal fibroblasts [40, 41]. Using lamps (UVA-340) that closely mimicked sun UV emission, Zigang

Dong's team showed that SUV–induced skin cancer relies upon activation of p38α, EGFR and PI3K signaling pathways [42, 43].

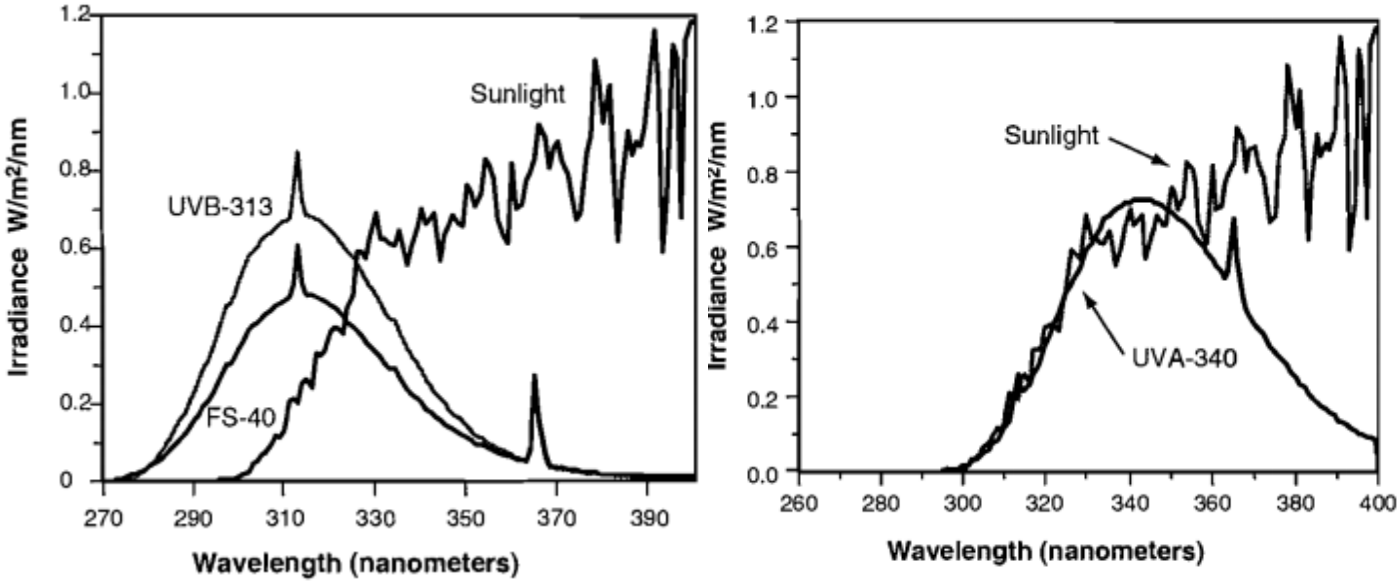

Figure 1.5 Spectral irradiance of commercial UVA and SUV lamps versus natural sunlight

Left graph shows the spectral energy distribution of the UVB lamp compared to sunlight. The UVB lamps showed a far greater disparity with sunlight bemuse of the far greater intensity of their range, while the SUV lamps (UV-A 340) were in good agreement with the daylight figures [44].

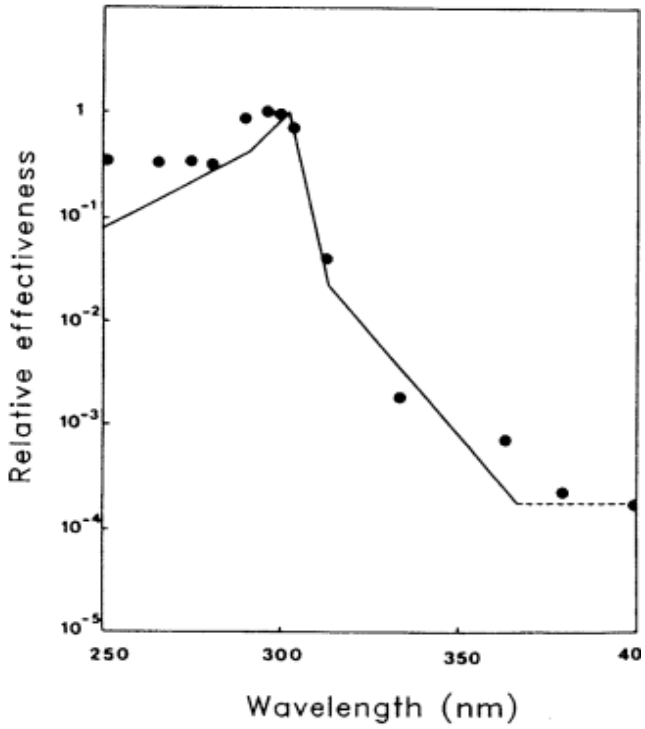

Figure 1.6 Sterenborg-Slaper action spectrum for ultraviolet-induced skin carcinogenesis in albino hairless mice

Effectiveness is defined as the reciprocal of the daily dose at each wavelength that leads to tumors of 1mm diameter in 50% of animals in 265 days, relative to the corresponding value at the wavelength of maximal effectiveness. The effectiveness between 340 and 400 nm represents an average value for that wavelength range.

From van der Leun (1987a)

1.4 IFNγ Signaling Pathway

Interferons (IFNs) are pleiotropic cytokines that mediate anti-viral responses, inhibit proliferation and participate in immune surveillance and tumor suppression by inducing the transcription of a number of IFN-stimulated genes. The IFN family includes two main classes of related cytokines, type I IFNs and type II IFN. There are many type I IFNs including IFNα, IFNβ and many others. By contrast, there is only one type II IFN, IFNγ that is produced by activated T cells, natural killer (NK) cells and dendritic cells. Its origin can be traced back more than 450 million years ago and its structure is conserved among vertebrates [45]. Not surprisingly, a deficiency or mutant form of IFNγ has a wide range of effects including an elevated risk to viral and bacterial infections.

IFNγ exerts its effects on cells by interacting with the specific IFNγ receptor that is composed of two subunits, IFNGR1 and IFNGR2 [46]. IFNγ receptor is expressed on surfaces of nearly all cells. JAK-STAT1 pathway plays a central role in IFNγ signaling [47]. Conventionally, IFNγ is associated with cytostatic/cytotoxic and antitumor mechanisms during cell-mediated adaptive immune response. However, more recent data have suggested a pro-tumorigenic role of IFNγ [48]. The IFNγ/STAT1 pathway has been extensively characterized as illustrated (Fig 1.7). Many of IFN-γ-regulated genes are in fact transcription factors (e.g., IRF1), which are activated by IFN-γ and are able to drive regulation of the next wave of transcription. STAT1:STAT1:IRF-9 heterodimers, ISGF3, and IRF1 are able to bind to IFN-stimulated response element (ISRE) promoter regions in target genes to regulate transcription. IRF1 is also able to promote transcription of STAT1 through an unusual ISRE site (IRF-E/GAS/IRF-E).

Ligand binding causes a conformational change in the IFNγR (IFNGR1; IFNGR2), such that the inactive JAK2 kinase undergoes autophosphorylation and

activation, which in turn allows JAK1 transphosphorylation by JAK2. The activated JAK1 phosphorylates functionally critical tyrosine on residue 440 of each IFNGR1 chain to form two adjacent docking sites for the SH2 domains of latent STAT1. The receptor-recruited STAT1 pair is phosphorylated near the C terminus at Y701. Phosphorylation induces dissociation of a STAT1 homodimer from the receptor. To a lesser extent, IFN-γ signaling also produces STAT1:STAT1: IRF-9 and STAT1:Stat2:IRF-9 [IFN-stimulated gene factor 3 (ISGF3)] complexes. STAT1 homodimers travel to the nucleus and bind to promoter IFN-γ-activation site (GAS) elements to initiate/suppress transcription of IFN-γ-regulated genes [49].

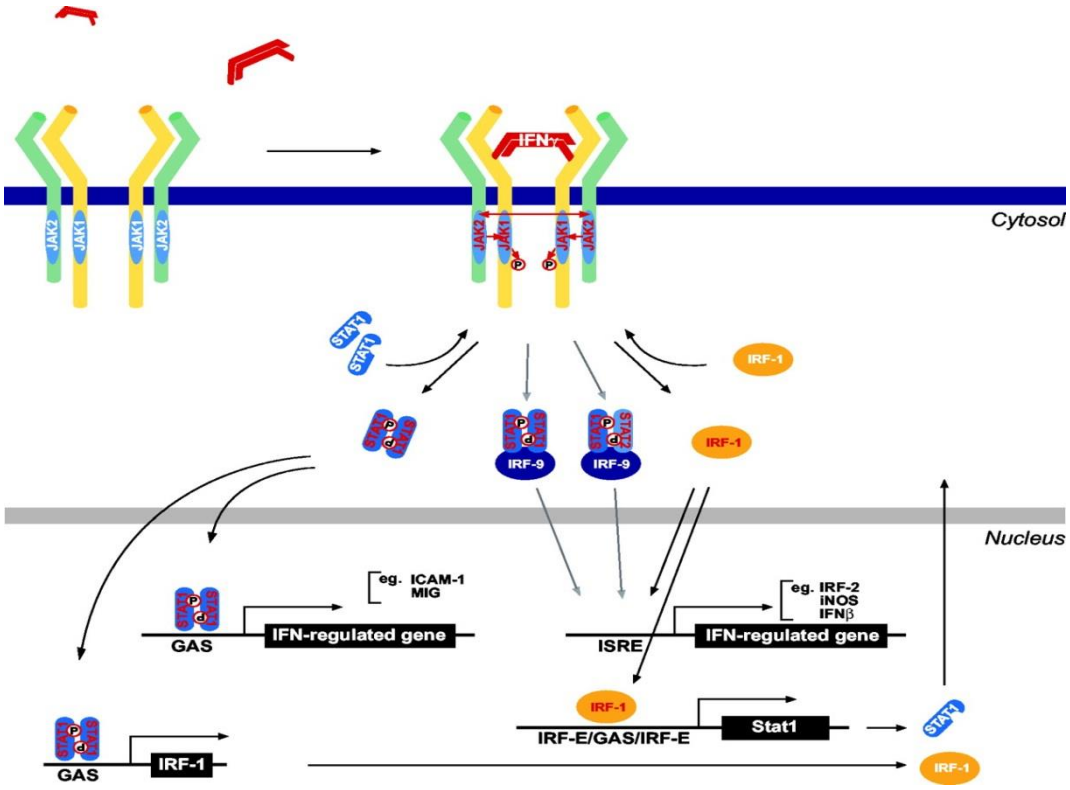

Figure 1.7 The current paradigm of canonical IFNγ/STAT1 signaling pathway Binding of IFNγ to the extracellular portion of the JAK receptor propagates an intracellular signaling cascade via IRFs and STATs. These activated proteins are able to translocate into the nucleus to successfully activate transcription of downstream targets [49].

1.5 Two Faces of STAT1 and IFNγ

STAT1, as the first discovered member of the STAT family, serves as the principal mediator of both type I and type II interferon activation [50]. Due to impaired IFN signaling, STAT1 deficient mice are highly susceptible to both viral and bacterial infection [51]. Activated STAT1 (p-STAT1) has been associated with anti-tumorigenic or tumor suppressive properties by modulating key components of immune tumor surveillance [50, 52, 53], inducing pro-apoptotic regulators such as Fas/FasL and caspases and by regulating negative cell cycle proteins such as p21 and p27 [54-56] as well as negatively regulating angiogenesis [57]. Beyond immune surveillance, STAT1 limits tumor growth in a cell-autonomous fashion [58, 59]. Studies have also revealed that the expression of STAT1 is frequently lost in various types of human cancer such as breast cancer, head and neck cancer, multiple myeloma and leukemia [60]. Researchers reported that following a single dose of the carcinogen methylcholanthrene, IFNγR$^{-/-}$ and STAT1$^{-/-}$ mice were highly susceptible to tumor formation compared 129/Sv controls. They also reported that STAT1 and p53 double knockout mice developed tumors more rapidly and with greater frequency than p53 single knockout mice [61]. STAT1-deficient mice spontaneously develop estrogen receptor α-positive luminal mammary carcinomas [62].

More recently, however, a pro-tumorigenic role of IFNγ/STAT1 has been demonstrated and discussed [48, 63, 64]. Constitutive activation of STAT1 and overexpression of IFNγ-related genes to breast cancers were associated with poor prognosis and activated STAT1 may confer resistance to radiation and adjuvant cancer therapy [65-69]. A pro-tumorigenic role of STAT1 has also been suggested in colon cancer [70, 71], esophageal squamous cell carcinoma [72], leukemia [73, 74] and melanoma [75]. Emerging evidence has inspired the new concept that

IFNγ/STAT1 may exhibit both tumor suppressive effects as well as pro-tumorigenic effects depending on the tissue milieu and stimuli.

Another interesting finding about IFNγ is that sustained low expression of IFNγ promoted tumor development whereas sustained high expression of IFNγ mediates significant antitumor effect. [76]. One intriguing underlying mechanism for IFNγ to promote tumorigenesis is by promoting tumor evasion of the immune system. PD-L1 and IDO are two downstream targets of IFNγ/STAT1 signaling pathway that can negatively regulate immune response in the local microenvironment. Merilino and his colleagues discovered that IFNγ links ultraviolet radiation to melanomagenesis in neonatal mice but not adult mice by promoting melanocytic cell survival/immunoevasion [77]. In the past few years, the importance of immune evasion, that exhibits dependence on IDO and PD-1/PD-L1, in tumor development has been established in SCC [78, 79] and melanoma [80, 81].

1.6 Rationale, Hypothesis and Specific Aims

Using the two stage carcinogenesis model, we have recently discovered that STAT1 is absolutely required for tumor promotion in the epidermis by CHRY and the activation of STAT1 in the epidermis is dependent on IFNγ signaling pathway [82]. CHRY treatment led to upregulation of unphosphorylated STAT1 at later time points and upregulation of interferon regulatory factor 1 (IRF1) mRNA and protein, which was dependent on STAT1 activation. Further analyses demonstrated that topical treatment with CHRY upregulated IFNγ mRNA in the epidermis and that the induction of both IRF1 and STAT1 was dependent on IFNγ signaling. $STAT1^{-/-}$ mice were highly resistant to skin tumor promotion by CHRY. These studies not only define a novel mechanism associated with skin tumor promotion by the anthrone

class of tumor promoters (e.g. CHRY) involving upregulation of IFNγ signaling in the epidermis, but also add new evidence to support the positive correlation between the upregulation of IFNγ/STAT1 signaling pathway and skin cancer promotion.

Induction of ROS is believed to play a significant role in the effects of SUV radiation on cellular processes including activation of cellular signaling pathways [83-85]. Thus, a common ROS-mediated mechanism may be shared by certain tumor promoters (e.g. CHRY and SUV) that activate multiple signaling pathways including the novel IFNγ/STAT1 pathway presented herein.

In this study, I have tested the hypothesis that SUV activates STAT1 in keratinocytes via an IFNγ signaling pathway.

Further study of this IFNγ/STAT1 signaling pathway in the context of skin homeostasis and in particular SUV-mediated skin carcinogenesis will likely lead to new targets and mechanisms for skin cancer prevention, especially for prevention of non-melanoma skin cancer.

The specific aims of this study are:

1. **Specific Aim 1: Examine the response of epidermal keratinocytes to IFNγ treatment.**
   Given that different types of cells respond to IFNγ uniquely; it is important to establish the *in vitro* response pattern of mouse keratinocytes after recombinant mouse IFNγ treatment.

2. **Specific Aim 2: Determine whether SUV (combination of UVA and UVB by a ratio of 15:1) activates IFNγ/STAT1 signaling in epidermis.**
   In this aim, I will determine whether SUV induces IFNγ signaling activation in mouse epidermis. Mice deficient for STAT1 in epidermal keratinocytes or deficient for IFN receptor 1 (IFNγR1) will be used. A method that can prevent

the activation of IFNγ signaling pathway in the skin will also be developed.

3. **Specific Aim 3: Determine the cells in the epidermis that produce IFNγ in response to CHRY and SUV.**

   The cellular source of IFNγ in the epidermis will be determined by employing IFNγ-reporter mice that carry an IRES-eYFP reporter cassette inserted between the translational stop codon and 3' UTR/polyA tail of the IFNγ gene.

Chapter 2. Materials and Methods

Animals

STAT1$^{-/-}$ mice were a generous gift from Dr. David Levy (Kaplan Cancer Center, New York School of Medicine, NY). A functionally null STAT1 allele was generated by deleting a portion of the protein-coding region, resulting in the loss of a portion of the DNA binding domain. These mice were backcrossed for at least 5 generations onto the FVB/N background. STAT1$^{flox/flox}$ mice were kindly provided by Dr. Mathias Müller and they were backcrossed for at least 5 generations onto the FVB/J background. The FVB background is a sensitive genetic background for two stage carcinogenesis experiments [86]. BK5.Cre transgenic mice were crossed with STAT1$^{flox/flox}$ mice to generate BK5.Cre x STAT1$^{flox/flox}$ mice, which are hereafter referred to as skin specific STAT1 deficient mice. Wild-type FVB mice, IFNγR1$^{-/-}$ mice and IFNγ-IRES-eYFP mice were purchased (The Jackson Laboratory). Genotyping was performed following standard protocol and primers used for genotyping were listed (Table 2.1).

Treatment

Chrysarobin was synthesized in our lab and dissolved in acetone to obtain a concentration of 220 nmol. The mice were used for experimentation at 6-8 weeks of age. The dorsal skin of each mouse was shaved 2 days prior to treatment. For multiple treatment with chrysarobin, mice received application once weekly for four weeks and were sacrificed at various time points after the last treatment. Acetone vehicle (0.2 mL) was used as a control.

SUV was emitted in a chamber containing 12 Sylvania F20T12/350BL lamps. The mice were shaved on their dorsal regions 2 days prior to treatment. During

treatment, each mouse was kept in individual enclosed cells with plastic cover allowing the transmission of SUV during the treatment. The enclosed mice were placed on a rotating platform that ensures even exposed doses. The mice were treated every other day for four times and each application took 4.5 hours to reach the dose of 28 J/cm^2 UVA+1.9 J/cm^2 UVB

Cell Culture

Non-tumorigenic keratinocyte C50 cells were cultured in EMEM-3 medium with non-essential amino acids. Cells were starved for 24 hours in MEM-2 in the absence of all growth factors. Cells were pretreated with or without JAK1/JAK2 inhibitor Ruxolitinib or JAK2 inhibitor AZD1480 (Selleck Chemicals) for 30min. In one protocol, the starvation medium that contains inhibitors was washed away before incubation with mouse recombinant IFNγ (BD Bioscience). In another protocol, stimulation with IFNγ started in the starvation medium that contained inhibitors. Cell were then lysed with cold RIPA buffer (Cell Signaling Technology) or RLT buffer (Qiagen) at various time points post stimulation.

Western Blot

After the mice were sacrificed by cervical dislocation, the dorsal skins were treated with a depilatory agent Nair (Church & Dwight Co.) followed by washing. Protease inhibitor cocktail, phosphatase inhibitor cocktail 2 and phosphatase inhibitor cocktail 3 (Sigma-Aldrich) were added to the RIPA lysis buffer (Cell Signaling Technology). After homogenization and centrifugation of the epidermal tissue lysate, the protein concentration of the supernatant was measured by Bio-Rad protein assay system (Bio-Rad Laboratories). Epidermal lysates, cultured cell lysates or immunoprecipitates were separated on SDS-PAGE under reducing condition. The separated proteins were then transferred onto nitrocellulose

membranes (Bio-Rad Laboratories). Membranes were blocked for 1 hour in 3% bovine serum albumin at room temperature followed by overnight incubation with specific primary antibodies (Table 2.2) at 4°C. After washing with TBST containing 0.1% Tween-20, blots were subjected to horseradish peroxidase-conjugated secondary antibodies (Table 2.2). After washing, the protein bands were visualized using a chemiluminescence detection kit (Pierce ECL Western Blotting Substrate). Quantitation was calculated by Image Studio Lite using Actin as the internal control.

Primary antibodies against the following proteins were used: STAT1, STAT3, Akt, p38, Erk, JNK1/2, c-Jun, IRF1, NFkB, p-STAT1^{Y701}, p-STAT1^{S727}, p-STAT3^{Y705}, p-Src^{T416}, JNK1/2$^{T183/Y185}$, p-c-Jun^{S73}, p-p38$^{T180/Y182}$, p-Erk1/2$^{T202/Y204}$, p-Akt^{T308}, p-Akt^{S473}, p-NFkB^{S536}, Bcl-xL and survivin (Cell Signaling Technology); Cox2 (Cayman); Actin (Sigma-Aldrich).

Quantitative RT-PCR

The epidermal tissue was homogenized in RLT buffer (Qiagen) before snap freezing. The total RNA was extracted using RNeasy Mini Kit (Qiagen) and residual genomic DNA was removed by treatment with RNase-free DNase I (Invitrogen). The concentration was determined by NanoDrop 2000c. 2 μg of total RNA was used to synthesize 20 μL of cDNA with High Capacity cDNA Kit (Applied Biosystems). The cDNA was diluted to 120 μL and 2 μL was used for each qPCR reaction. The reaction was performed using specific primers (Table 2.2) and iTaq SYBR green master mix (Bio-Rad Laboratories) on the Applied Biosystems ViiA 7. Relative gene induction was calculated using comparative Ct method with GAPDH used as an internal control.

Immunofluorescence Staining

The dorsal skins were fixed for 10 min in 4% paraformaldehyde before sinking

in 30% sucrose for another 10 min. Tissues were then embedded into FSC22 OCT (Surgipath Medical Industries) and snap frozen by liquid nitrogen. The 10 μm cryostat sections were permeabilized by 0.2% Triton-X100 and blocked by 1% bovine serum albumin and 10% serum. Sections were stained with specific primary antibody overnight at 4°C before washing with PBST. After incubation with fluorochrome (Alexa Fluor 488 or Alexa Fluor 594)-conjugated secondary antibodies for 2 hours at room temperature, the sections were washed and mounted using VECTASHIELD anti-fade mounting medium with DAPI (Vector Laboratories). Images were analyzed using an Olympus DP70 fluorescence microscope

Primary antibodies against CD3 and GFP (Abcam) were used for immunostaining.

Histological Analysis

The excised dorsal skins were fixed in 10% neutral-buffered formalin. The formalin-fixed paraffin-embedded samples were sectioned and stained with hematoxylin & eosin, Ki67, cleaved caspase 3 and CD31 by the histology core at Dell Pediatric Research Institute, the University of Texas at Austin.

Flow Cytometry Analysis

Excised dorsal skins were subjected to a modified primary keratinocyte protocol [87]. After mechanically removing the subcutaneous fat, the skins were incubated in 5 mg/mL dispase (Life Technologies) at 37 °C for 30 min. Subsequently, the epidermis was peeled gently, incubated in 1 mg/mL collagenase IV (Sigma-Aldrich) at 37 °C for 30 min and strained through a 40 μm cell strainer to obtain a single cell suspension. The mononuclear cells including lymphocytes were separated from keratinocytes by Ficoll-Paque Plus (StemCell Technologies).

PE-Cy7 anti-CD3e (eBioscience) were used for extracellular staining and Zombie Violet Dye (Biolegend) was used for validation of cell viability. The samples were permeabilized and fixed by a Cytofix/Cytoperm Plus Kit (BD Pharmingen) before intracellular staining with APC anti-IFNγ or APC IgG1 Isotype control (BD Pharmingen). Spleenocytes were collected and stimulated with cell stimulation cocktail (eBioscience) containing TPA and ionomycin, and Brefeldin A (eBioscience) to prepare single color control. Brefeldin A was also added in every step during the isolation. The samples were finally analyzed by a BD LSRFortessa flow cytometry and FlowJo software.

Oligonucleotides Application

Double-stranded oligonucleotides were synthesized (Integrated DNA Technologies) from complementary single-stranded phosphorothioate bonded oligonucleotides. For decoy treatment of 50 nmol on one mouse, 1.45 g ointment was prepared by homogenizing 1240 mg Vaseline, 65 mg stearyl alcohol and 725 nMole oligonucleotides in 145 µL TEN buffer (10 mM Tris and 1 mM EDTA and 150 mM NaCl). All solutions and the ointment base, pestles, and mortars were pre-warmed to 37°C before stirring for at 37°C for 15min during the mix. After the ointment cooled down, 1 mL of the ointment was painted topically for each application. Ointment was applied topically one day before chrysarobin treatment.

STAT1 decoy 5'- **CATG**TTATGCATATTCCTGTA**AGTG** -3'

STAT1 mutant 5'- **CATG**TTATGCAGACCGTAGTA**AGTG** -3'

The bold letters denote phosphorothioate-bonded bases.

Statistical Analyses

For comparisons of quantitative protein expression, relative gene expression, epidermal thickness, labeling index and positive stained cells, the Mann-Whitney

U test was used. If not stated, significance was set at $p<0.05$. The statistical analyses were performed on JMP software.

STAT1$^{-/-}$		Expected Fragments
ST1	GAGATAATTCACAAAATCAGAGAG	WT 142 bp
ST2	CTGATCCAGGCAGGCGTTG	KO 342 bp
ST3	TAATGTTTCATAGTTGGATATCAT	
IFNγR1$^{-/-}$		
oIMR6916	CTTGGGTGGAGAGGCTATTC	WT 189 bp
oIMR6917	AGGTGAGATGACAGGAGATC	KO 280 bp
oIMR0587	CCCATTTAGATCCTACATACGAAACATACGG	
oIMR0588	TTTCTGTCATCATGGAAAGGAGGGATACAG	
STAT1$^{flox/flox}$		
69fwd	GACATCTGGGGCAACTAGATA	WT 522 bp
54rev	CTGGCATTTCTCCCTCACAC	FL 357 bp
77rev	CTCACACCTACCCCTGTCG	
78fwd	GGTGAAATTGCAAGAGCTGA	
BK5.Cre x STAT1$^{flox/flox}$		
52fwd	TTGGGCGTCACACATTACAT	WT 482 bp
54rev	CTGGCATTTCTCCCTCACAC	Floxed 830 bp
71fwd	CCAGAAGGCCACCTACAGAA	
BK5.Cre		
Crefwd	CCATCTGCCACCAGCCAG	Cre 281 bp
Crerev	TCGCCATCTTCCAGCAGG	

Table 2.1 Primer sequences for genotyping

Gene	**Forward Primer**	**Reverse Primer**
Cxcl9	TCCTTTTGGGCATCATCTTC	TTCCCCCTCTTTTGCTTTTT
Cxcl10	CCGGGGTGTGTGCGTGGCTTCA	TGCGAGCCTATCCTGCCCACGTG
Cxcl11	AGGAAGGTCACAGCCATAGC	CGATCTCTGCCATTTTGACG
Cox2	CAAGACAGATCATAAGCGAGGA	GGCGCAGTTTATGTTGTCTGT
GAPDH	CATGGCCTTCCGTGTTCCTA	TGTCATCATACTTGGCAGGTTTCT
IFNβ	ACACTGCCTTTGCCATCCAAGAG	TCCACCCAGTGCTGGAGAAATTG
IFNγ	CCTTCTTCAGCAACAGCAAGGC	GGGTTGTTGACCTCAAACTTGGC
iNOS	ACCTTGTTCAGCTACGCCTT	CATTCCCAAATGTGCTTGTC
IRF1	AATTCCAACCAAATCCCAGG	AGGCATCCTTGTTGATGTCC
PD-L1	GTGAAACCCTGAGTCTTATCC	GACCATTCTGAGACAATTCC
STAT1	TCCCGTACAGATGTCCATGAT	CTGAATATTTCCCTCCTGGG

Table 2.2 Primer sequences for RT-qPCR

Chapter 3: Examination of the IFNγ/STAT1 Signaling Axis in C50 Keratinocytes

It has been well documented that IFNγ can trigger various responses in different cell types [88]. C50 cells, a non-tumorigenic keratinocyte cell line was used to characterize how keratinocytes respond to IFNγ stimulation at molecular level (Fig. 3.1). With recombinant mouse IFNγ treatment, STAT1 was phosphorylated at Y701 very rapidly, with an observed increase of IRF1 beginning at 3h, followed by a prolonged increase of uSTAT1. Not quite consistent with the paradigm of IFNγ/STAT1 pathway, phosphorylation of STAT3 at Y705 was also observed. It was reported that p-Src was the kinase that phosphorylated STAT3 following IFNγ treatment in mouse embryonic fibroblasts [89]. The level of p-Src after IFNγ treatment in our experiment did not increase until 6h post IFNγ stimulation. T Quantitative PCR has shown that Cxcl9/10/11 are the most responsive downstream targets following IFNγ treatment. Several pro-inflammatory downstream targets that were commonly associated with tumor promotion, including iNos, Cox-2 and PD-L1, also increased. These findings reconciled our understanding of how keratinocytes respond to IFNγ stimulation.

Though the importance of pSTAT3 in IFNγ pathway is unknown, we have discovered that JAK2 was responsible for the phosphorylation of both STAT1 and STAT3 (Fig. 3.2). Incubation with both JAK1/2 inhibitor Ruxolitinib and JAK2 inhibitor AZD1480 completely prevented the phosphorylation of STAT1 and STAT3, and the increase of downstream target IRF1, suggesting that JAK2 is the primarily kinase in IFNγ pathway that phosphorylates STAT1 and STAT3. Incubation with EGFR inhibitor AG490 did not prevent the phosphorylation of STAT1 and STAT3 by IFNγ treatment, indicating that this pathway circumvents

signaling through EGFR kinase (Data not shown). Pretreatment with JAK2 inhibitor for 30min significantly delayed the onset and extent of STAT3 phosphorylation, and to a lesser degree, STAT1 phosphorylation, indicating that JAK2 preferably phosphorylates STAT1 in the IFNγ signaling pathway. Immunoprecipitation data showed low level formation of pSTAT1:pSTAT3 heterodimer although the molecular consequences of that heterodimer are currently unknown (data not shown).

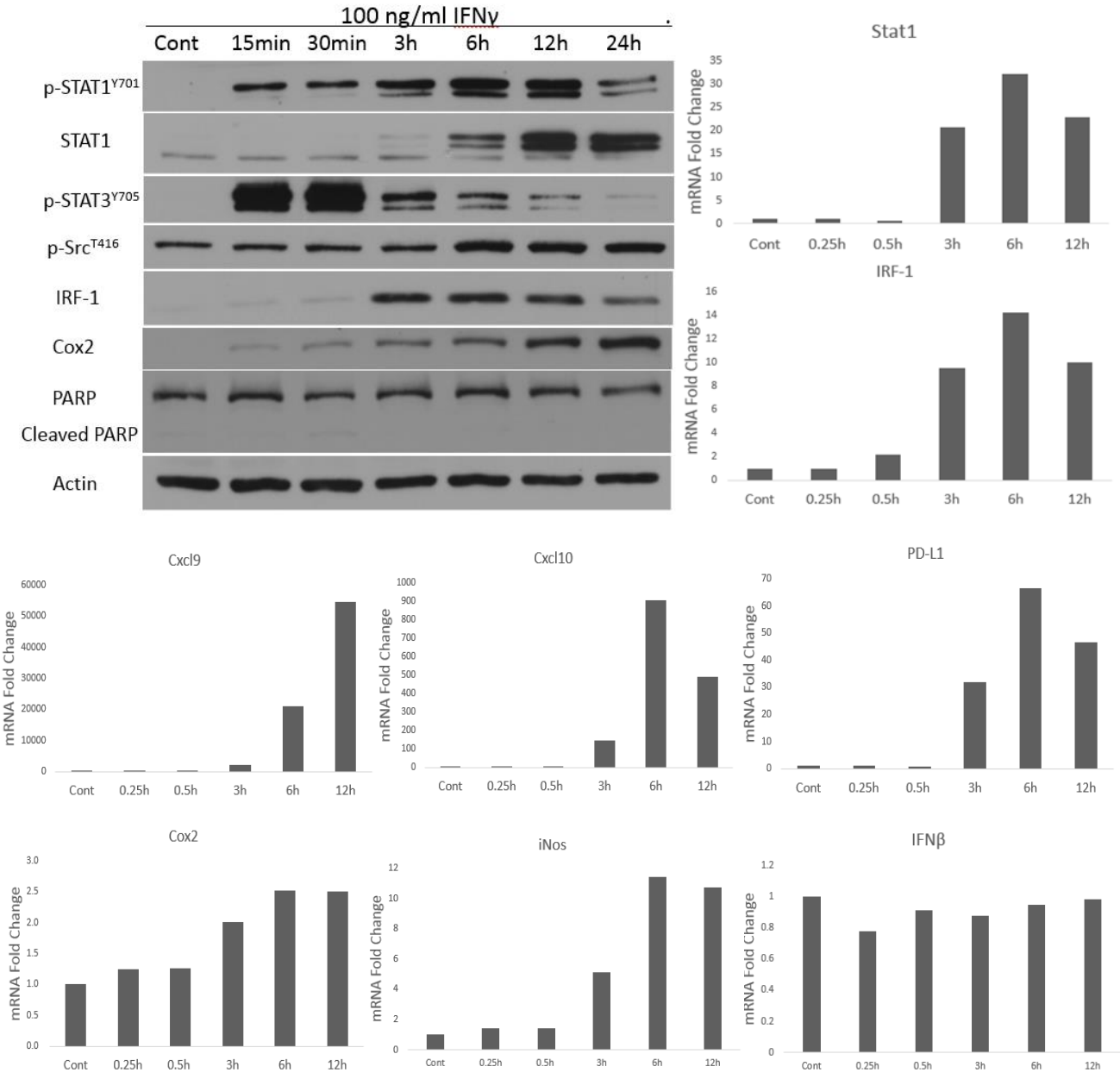

Figure 3.1 Examination of the IFNγ/STAT1 signaling pathway in C50 keratinocytes with IFNγ treatment

Serum starved C50 non-tumorigenic keratinocytes were stimulated with recombinant mouse IFNγ (100 ng/mL). Protein lysates and RNA were collected at indicated time points.

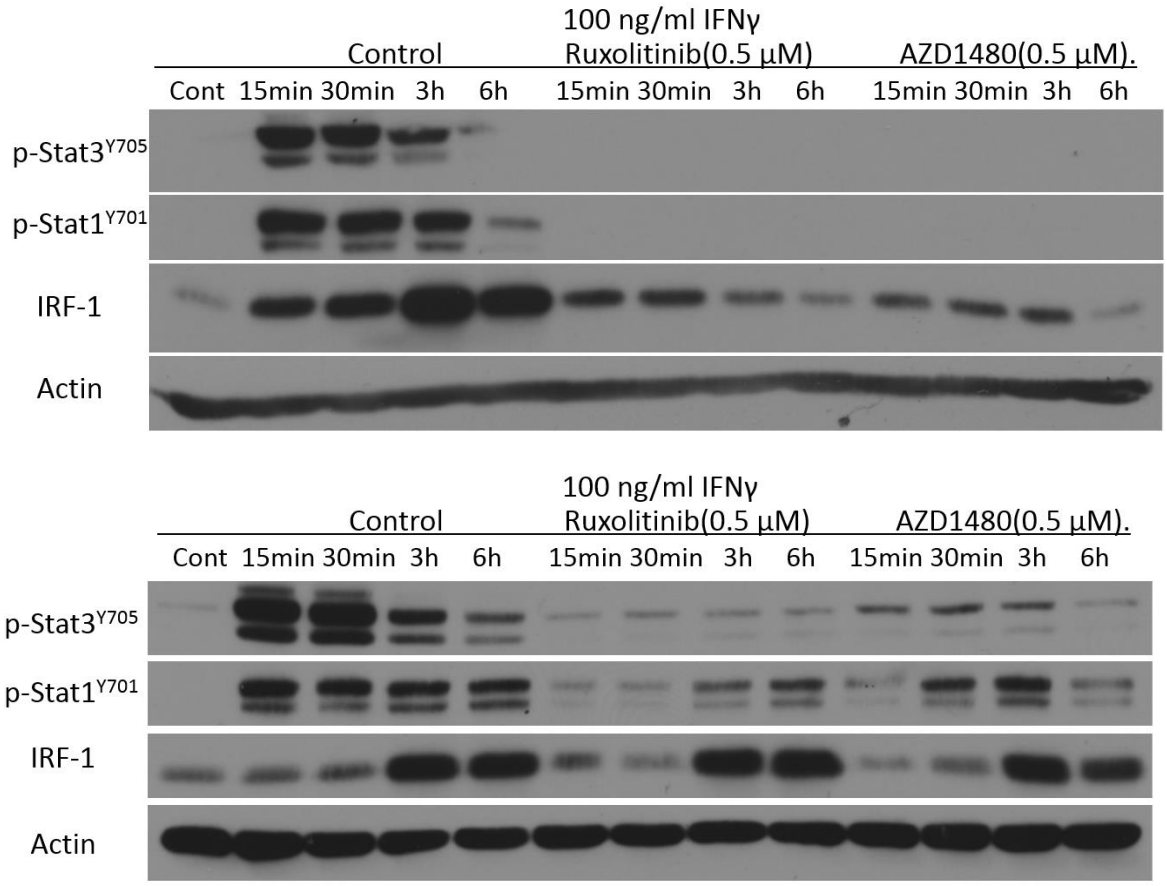

Figure 3.2 Evaluation of the effect of JAK inhibitors incubation or pretreatment on IFNγ/STAT1/IRF1 signaling axis in C50 keratinocytes with IFNγ treatment

Upper: Serum starved C50 non-tumorigenic keratinocytes were incubated with JAK1/JAK2 inhibitor Ruxolitinib or JAK2 inhibitor AZD1480 for 30min, and then stimulated with recombinant mouse IFNγ (100 ng/mL).

Lower: Serum starved C50 non-tumorigenic keratinocytes were pretreated with JAK1/JAK2 inhibitor Ruxolitinib or JAK2 inhibitor AZD1480 for 30min, and then stimulated with recombinant mouse IFNγ (100 ng/mL) in fresh medium without the presence of

Chapter 4. Examination of the IFNγ/STAT1 Signaling Pathway Following SUV Treatment

4.1 SUV Activated IFNγ/STAT1 Pathway in Wildtype Mice.

Previous experiments with CHRY have established a novel mechanism of skin tumor promotion. Investigations of the SUV activated IFNγ/STAT1 pathway may help us to evaluate our hypothesis that this mechanism is shared by more than one chemical tumor promotor, and that it has relevance to human skin cancer.

A time course of FVB/J mice with SUV treatment was conducted. Here, we clearly demonstrated that the IFNγ/STAT1 pathway was activated in adult mice after SUV treatment (Fig. 4.1). Phosphorylation of STAT1 at Y701 increased at 3h and gradually decreased after 12h following SUV treatment. A robust induction of uSTAT1 and IRF1 was also observed. qPCR data suggested that, compared to the untreated basal level, IFNγ mRNA levels increased by 3 folds in the epidermis at 1h following SUV treatment. The pattern of IFNγ pathway activation in the epidermis after SUV treatment was similar to what we have observed *in vitro* with IFNγ treatment (Fig. 3.1).

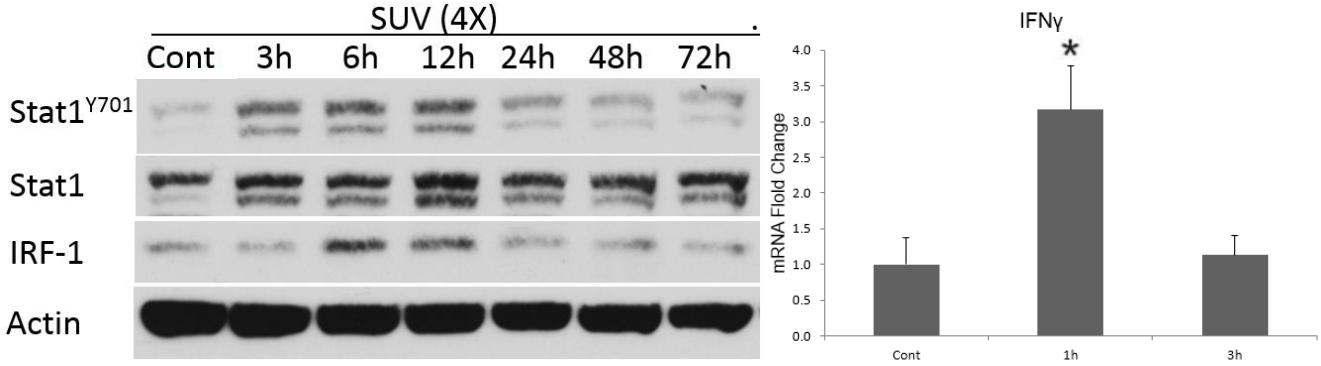

Figure 4.1 Examination of the IFNγ/STAT1/IRF1 signaling pathway in the epidermis of FVB/J mice with SUV treatment

FVB/J female mice were shaved and treated with SUV every other day for a total of four doses. Epidermal protein and RNA samples were collected at indicated time points after the last SUV treatment. * indicates value between experimental group and control group was significantly different by Mann-Whitney U-test ($p<0.05$).

4.2 The Activation of IFNγ Pathway by SUV Depended on STAT1 Activation and Intact IFNγ Receptor.

Multiple treatments of SUV administrated every other day for a total of 4 treatments led to phosphorylation of STAT1 at both Y701 and S727 at 6h, and an increase of IRF1 and uSTAT1, which all depended on a functional STAT1 as these changes were not observed in $STAT1^{-/-}$ mice (Fig. 4.2). All of these events suggested that IFNγ/STAT1 was activated in a similar manner in the epidermis as we have observed following treatment with CHRY [82].

To further test our hypothesis, IFNγR1-/- mice were utilized. As shown in Figure 4.3, a functional IFNγ receptor was required for the phosphorylation of STAT1 Y701 and the induction of IRF1 and uSTAT1 induced by SUV. mRNA levels of other downstream targets of this pathway were evaluated by qPCR and were found to be consistent with the changes at protein levels (Fig. 4.3). Chemokines, such as, Cxcl9, Cxcl10 and Cxcl11, were dramatically increased following SUV radiation and were also dependent on an intact IFNγR1 for maximal expression. An increase of Cox2 expression after SUV treatment was observed but did not appear to be primarily dependent on IFNγ signaling pathway.

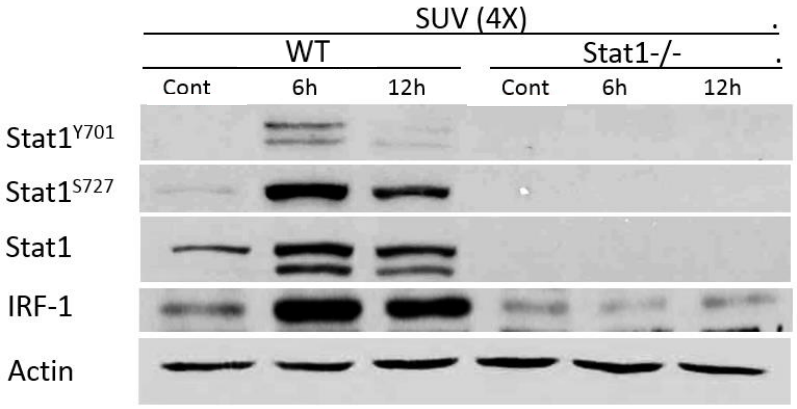

Figure 4.2 Analysis of STAT1 phosphorylation and IRF1 protein level following SUV treatment in STAT1 deficient mice

Female WT and STAT1$^{-/-}$ (4/group) were shaved and treated with SUV every other day for a total of four doses. Epidermal protein samples were collected at indicated time points after the last SUV treatment.

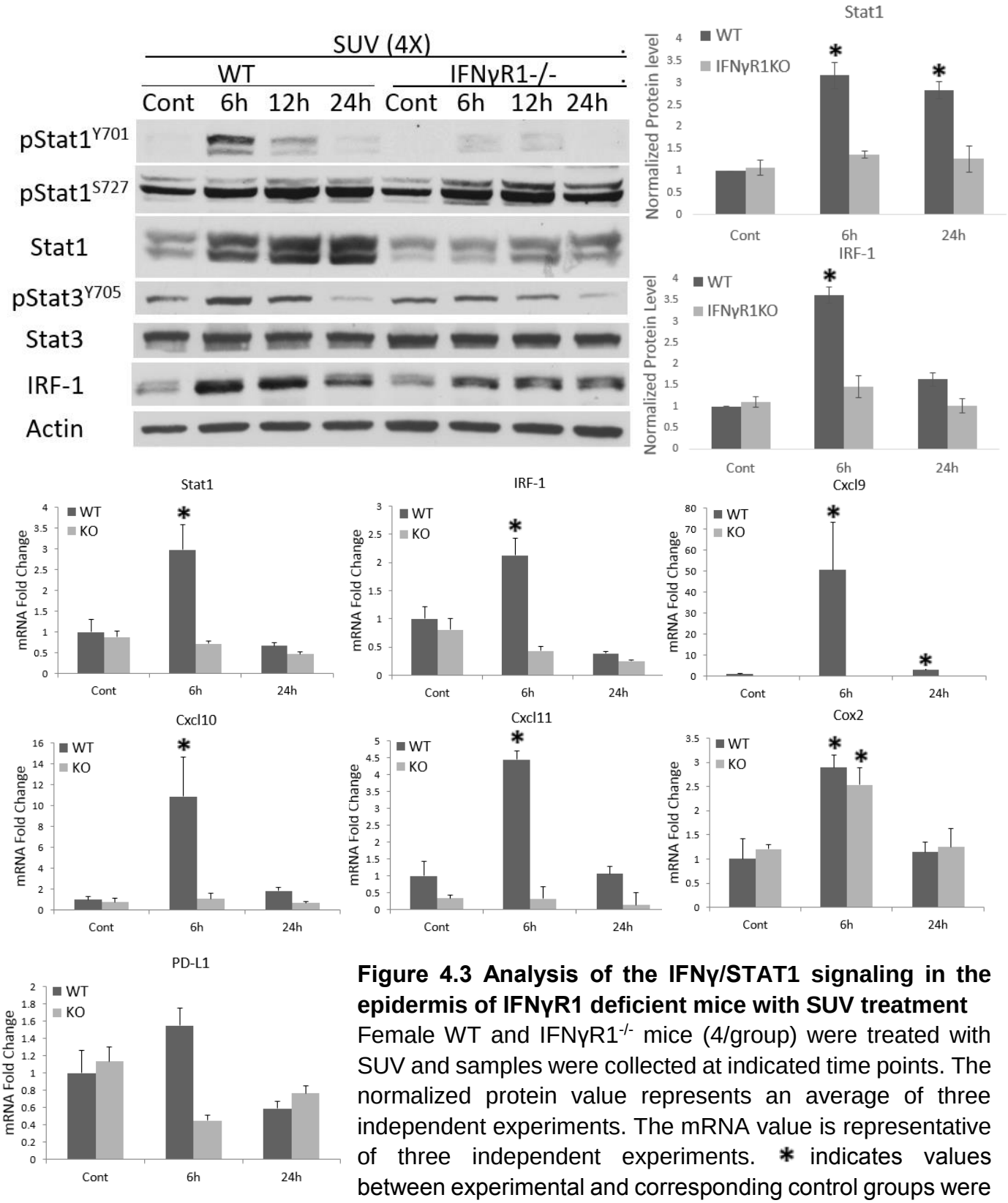

Figure 4.3 Analysis of the IFNγ/STAT1 signaling in the epidermis of IFNγR1 deficient mice with SUV treatment
Female WT and IFNγR1$^{-/-}$ mice (4/group) were treated with SUV and samples were collected at indicated time points. The normalized protein value represents an average of three independent experiments. The mRNA value is representative of three independent experiments. * indicates values between experimental and corresponding control groups were different by Mann-Whitney U-test ($p<0.05$).

4.3 The Impact of STAT1 Deficiency in Keratinocytes on IFNγ Pathway Induction

To further explore the role of IFNγ/STAT1 signaling in the epidermis, we employed keratinocyte specific STAT1 knockout mice. For these studies, BK5.Cre x $STAT1^{flox/flox}$ mice, where STAT1 is specifically knocked out in keratinocytes, were used. Initial experiments with four doses of CHRY treatment did not induce the activation of IFNγ pathway (Fig. 4.4) in BK5.Cre x $STAT1^{flox/flox}$ mice. This corroborates previous results using $STAT1^{-/-}$ mice from our laboratory and provides verification of the establishment of BK5.Cre x $STAT1^{flox/flox}$ mice model. In addation, these data strongly supported the conclusion that activation of this pathway in the keratinocytes was responsible for the obsereved effects. Notably, the production of IFNγ mRNA in the epidermis after chrysarobin treatment was not dependent on the presence of STAT1.

We next evaluated the effect of keratinocyte specific deletion of STAT1 on SUV induced IFNγ/STAT1 signaling. Compared to the data with $STAT1^{-/-}$ mice (Fig. 4.2), essentially identical results were obtained using BK5.Cre x $STAT1^{flox/flox}$ mice. These findings were validated at the transcriptional level by reverse quantitative PCR (Fig. 4.5). These data strongly suggested that SUV activated IFNγ/STAT1 pathway in the epidermis occurs in a similar way as the tumor promoter CHRY.

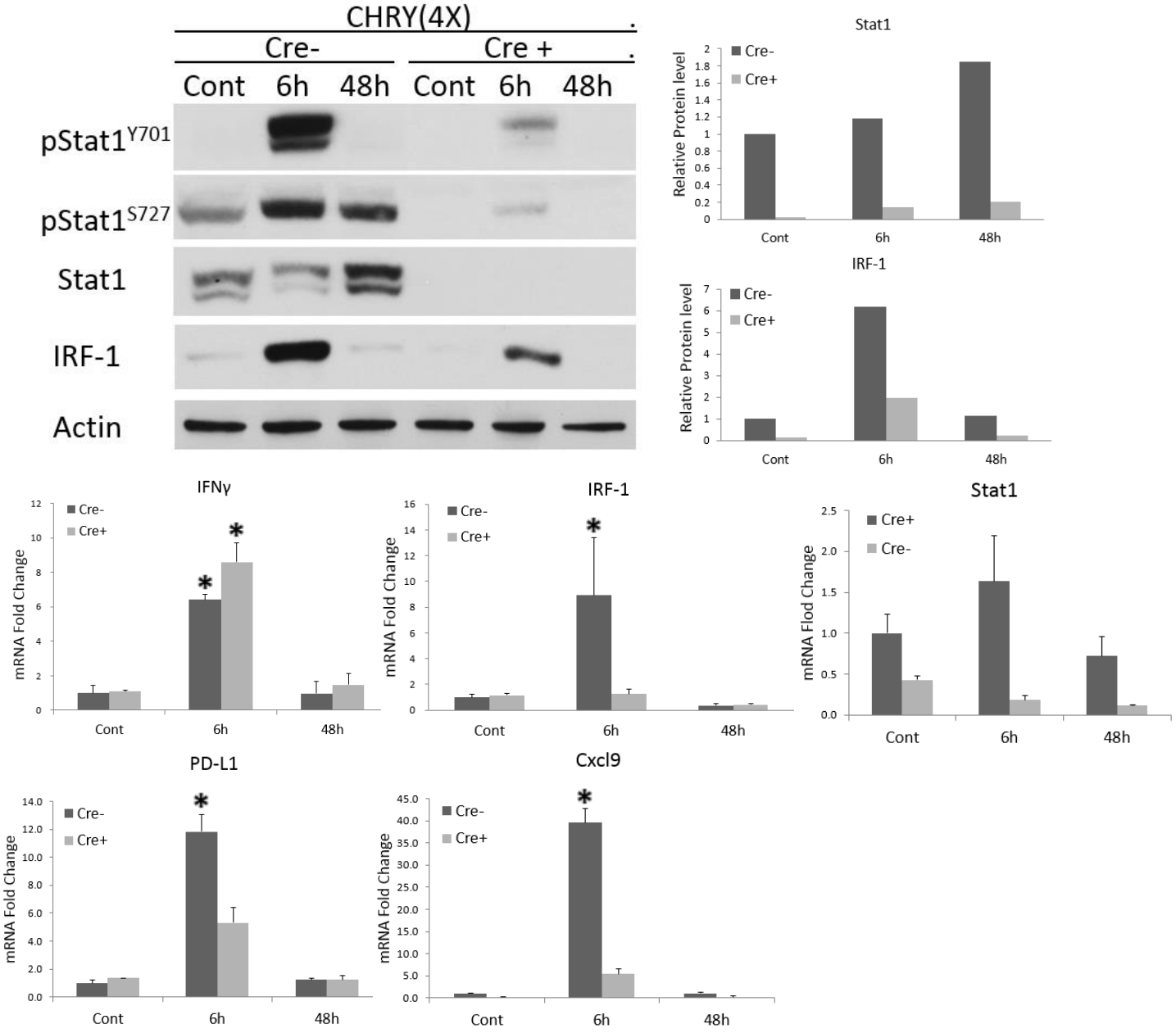

Figure 4.4 Examination of the IFNγ/STAT1/IRF1 signaling axis in response to CHRY treatment using mice with epidermal specific deletion of STAT1

STAT1$^{flox/flox}$ and BK5.Cre.STAT1$^{flox/flox}$ mice (4/group) received 220nmol chrysarobin weekly for four weeks. Epidermal lysates were prepared at the indicated time points for protein and mRNA analyses. * indicates values between experimental and corresponding control groups were significantly different by Mann-Whitney U-test ($p<0.05$). Relative protein value is an average of two independent experiments.

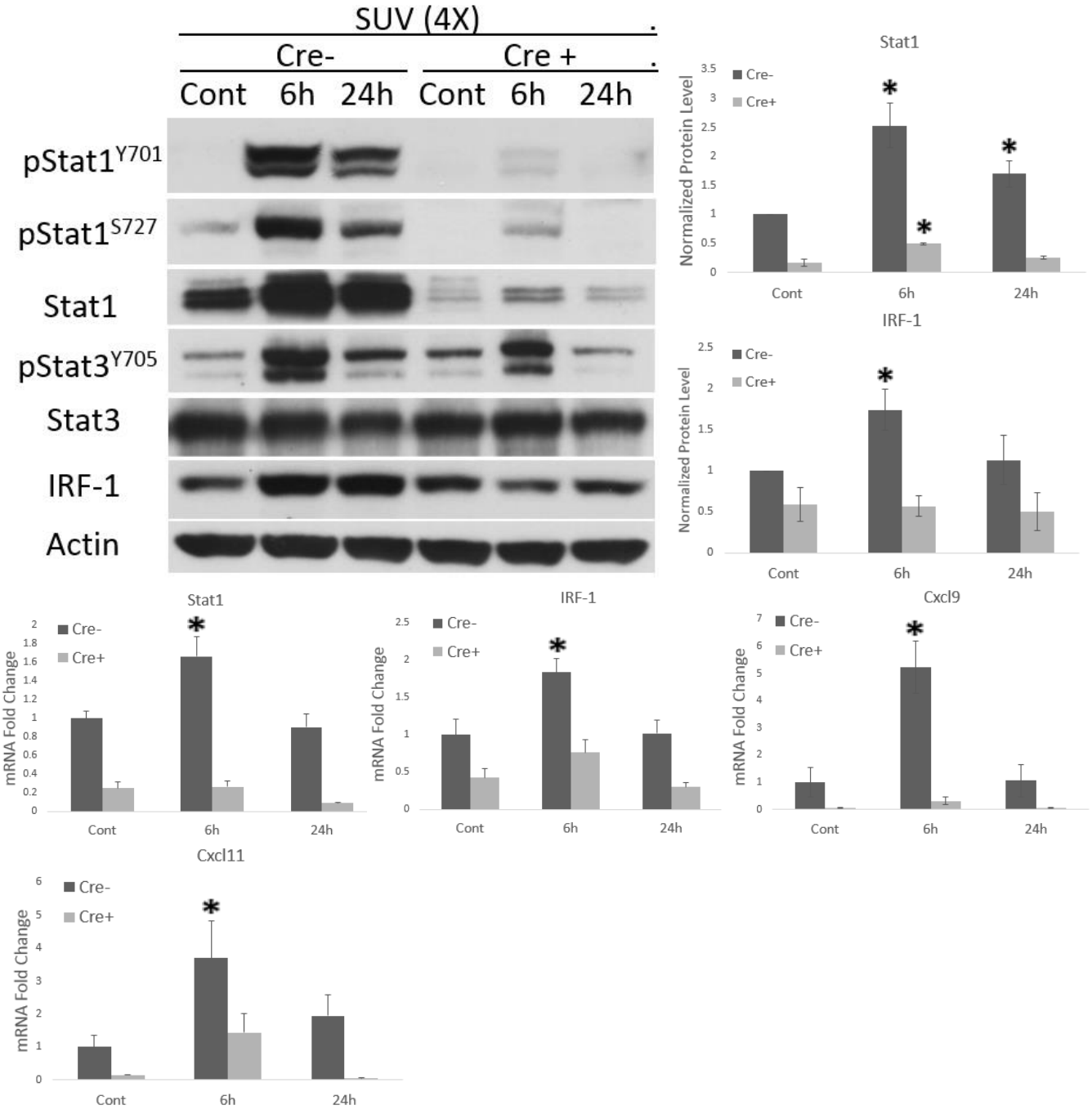

Figure 4.5 Examination of the IFNγ/STAT1/IRF1 signaling axis in response to SUV treatment using mice with epidermal specific deletion of STAT1

STAT1$^{flox/flox}$ and BK5.Cre.STAT1$^{flox/flox}$ mice (4/group) were treated with SUV every other day for a total of four doses and epidermal samples were collected at indicated time points. The normalized protein value represents an average of from three independent experiments. The quantitative mRNA value is a representative (4-6 mice/group) of three independent experiments. * indicates values between experimental and corresponding control groups were significantly different by Mann-Whitney U-test ($p<0.05$).

Chapter 5. Inhibition of IFNγ Pathway by Topical Treatment of Oligonucleotides

Decoy oligonucleotides are short double-stranded DNA molecules that penetrate the skin rather easily, presumably due to active transcellular transport. When targeting transcription factors, they mimic the genomic binding site of the target transcription factor so that its activity is blocked and, thereby, the expression of its target genes [90]. When targeting mRNA expression, antisense oligonucleotides hybridize with a target mRNA to downregulate gene expression via a RNase H-dependent mechanism [91, 92].

To target the transcription factor STAT1, a decoy strategy has been developed using oligonucleotides containing a gamma-activated site (GAS) motif for specific binding [93]. A Vaseline-based ointment was formulated for topical delivery of oligonucleotide decoys and stearyl alcohol was added as an emulsifier.

The decoy was applied in doses of 25 nmol and 50 nmol. Mutant decoy in which the consensus-binding GAS element has been mutated was prepared in 50 nmol. Topical treatment with decoy inhibited the activation of IFNγ pathway in a dose dependent manner (Fig. 5.1). Notably, decoy treatment substantially inhibited the induction of phosphorylated STAT1 and IRF1 after CHRY application, suggesting a mechanism of dephosphorylation associated with decoy oligonucleotides.

Interestingly, the induction of phosphorylated STAT3 (Fig. 5.1) and its downstream targets, including Bcl-xL and Survivin (Fig. 5.2), were not affected by the STAT1 decoy treatment, demonstrating a specificity of this STAT1 decoy strategy.

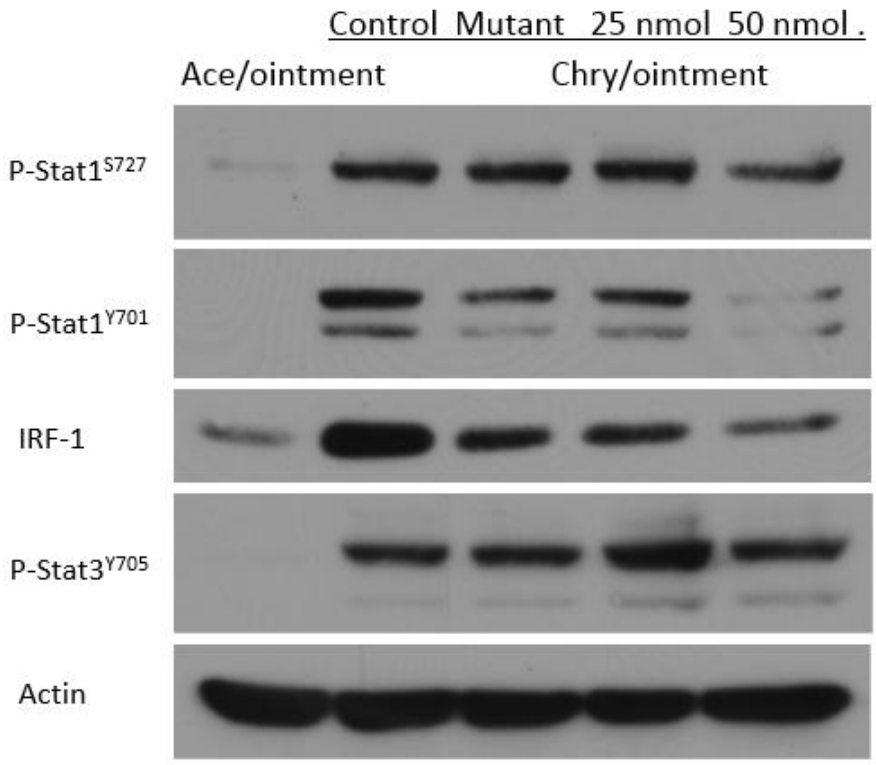

Figure 5.1 STAT1 decoy oligonucleotides mediated inhibition of IFNγ signaling pathway in FVB/J mice epidermis after challenge with CHRY

Female FVB/J mice (4 mice/group), 8 weeks old, were topically treated with ointment containing different doses of STAT1 decoy or mutant decoy 24h before challenge with CHRY. The treatment was applied weekly for three successive weeks. Six hours after the last CHRY challenge, epidermal protein samples were collected for analyses.

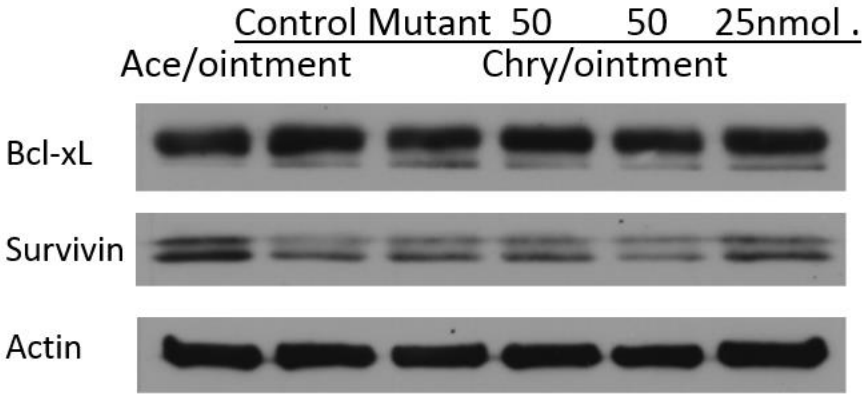

Figure 5.2 Specificity of STAT1 decoy oligonucleotides
STAT1 decoy oligonucleotides did not affect the induction of STAT3 downstream targets after CHRY treatment.

Chapter 6. The Cellular Source of IFNγ Production

Our data demonstrated that both CHRY and SUV treatment led to the upregulation of IFNγ mRNA and the activation of IFNγ pathway in the epidermis. Consequently, the cellular source of IFNγ was interrogated.

There is evidence that IFNγ may be produced by T cells, natural killer cells and natural killer T-cells. Also, there is considerable complexity in the immune cell content of the skin. The relative contribution and function of resident versus migrating cells still remains unclear in many instances.

We employed IFNγ reporter mice in this aim. The "interferon-gamma reporter with endogenous polyA transcript" allele has an IRES-eYFP reporter cassette inserted between the translational stop codon and 3' UTR/polyA tail of the IFNγ gene. Thus, the bicistronic IFNγ-IRES-eYFP mRNA is under control of the endogenous IFNγ promoter/enhancer regions with proper regulation defined by the endogenous 3' UTR and polyA tail.

The skin was fixed at 1 hour after SUV treatment and double immunofluorescence staining showed that CD3+ cells were the source of IFNγ in the epidermis and dermis (Fig. 6.1). It was also observed that SUV greatly induced epidermal hyperplasia and an infiltration of CD3+ cells into the dermis. However, the number of CD3+ cells in the epidermis significantly decreased with SUV treatment.

With chrysarobin treatment, CD3+ cells decreased in the epidermis while an infiltration of CD3+ cells in to the dermis was observed. CD3+ cells are the main source of IFNγ in the hyperplastic epidermis (Fig. 6.2 CHRY^{1st}) but not the only source (Fig. 6.2 CHRY^{2nd}). In the dermis, however, compared with acetone group, there was a significant increase of both eYFP+ and CD3+ cells following chrysarobin treatment. Most of the eYFP+ cells were not CD3+.

By using flow cytometry, we have confirmed that, in the epidermis, chrysarobin treatment led to the production of IFNγ from both CD3+ and CD3- cells by the ratio of 2:1 (Fig. 6.3).

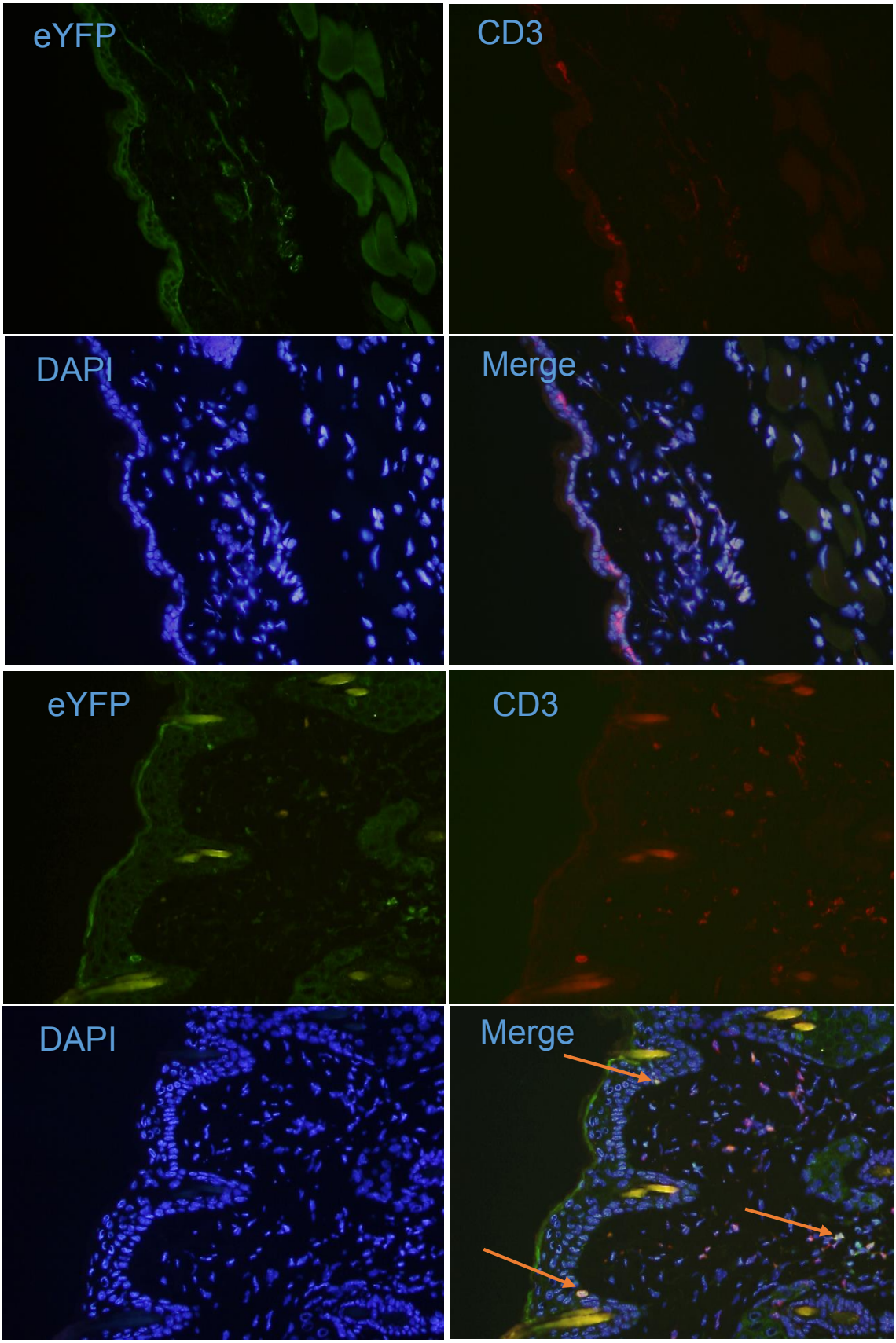

Figure 6.1 continued next page

Figure 6.1 Identification of IFNγ-producing CD3+ cells following SUV treatment
Female IFNγ reporter mice, 6 weeks old, were treated with SUV every other day for a total of four doses. Skin was collected at 1h following the last treatment. eYFP, CD3 and DAPI triple immunofluorescence staining were performed using 4% PFA fixed frozen sections.

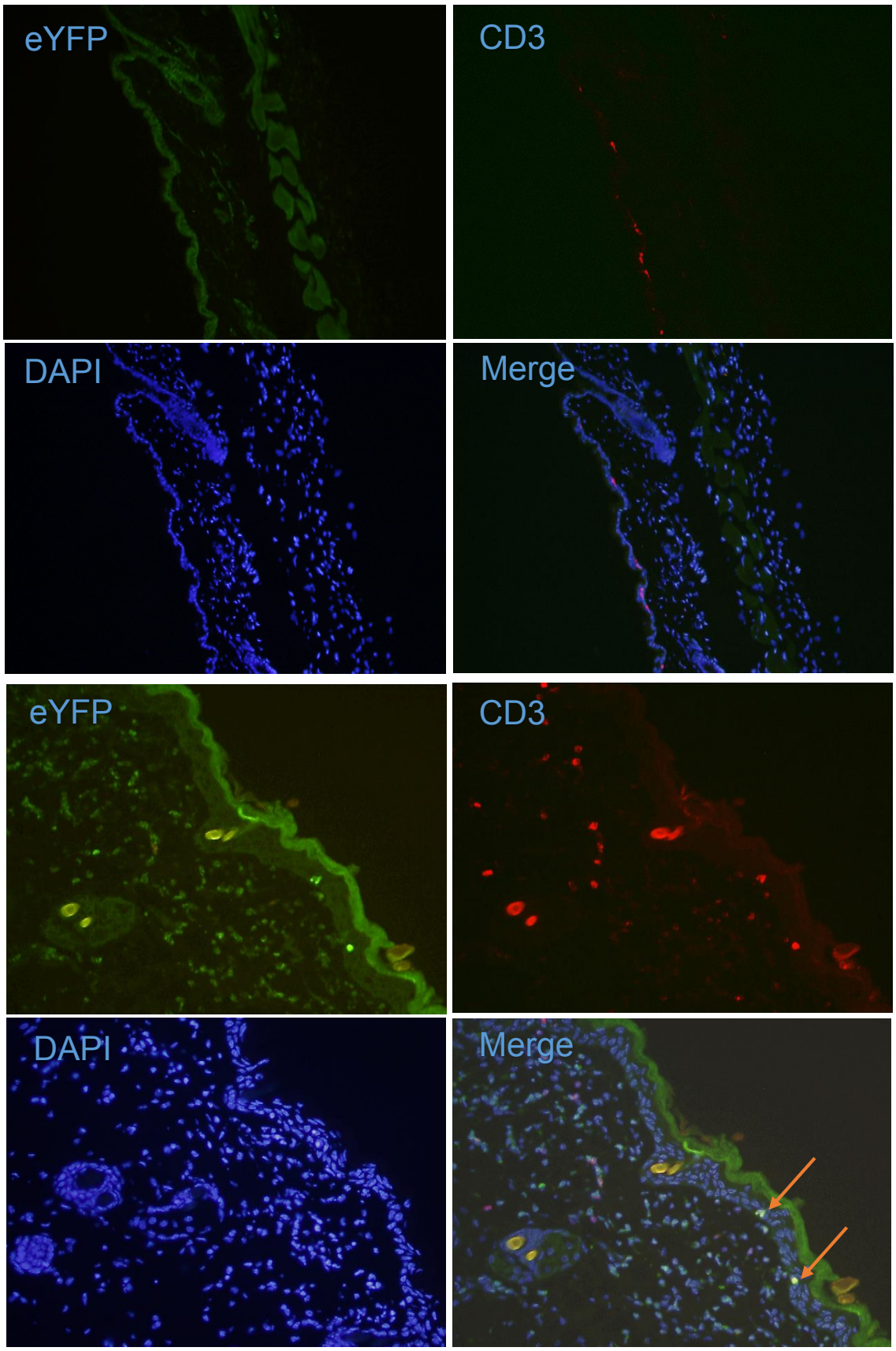

Figure 6.2 continued next page

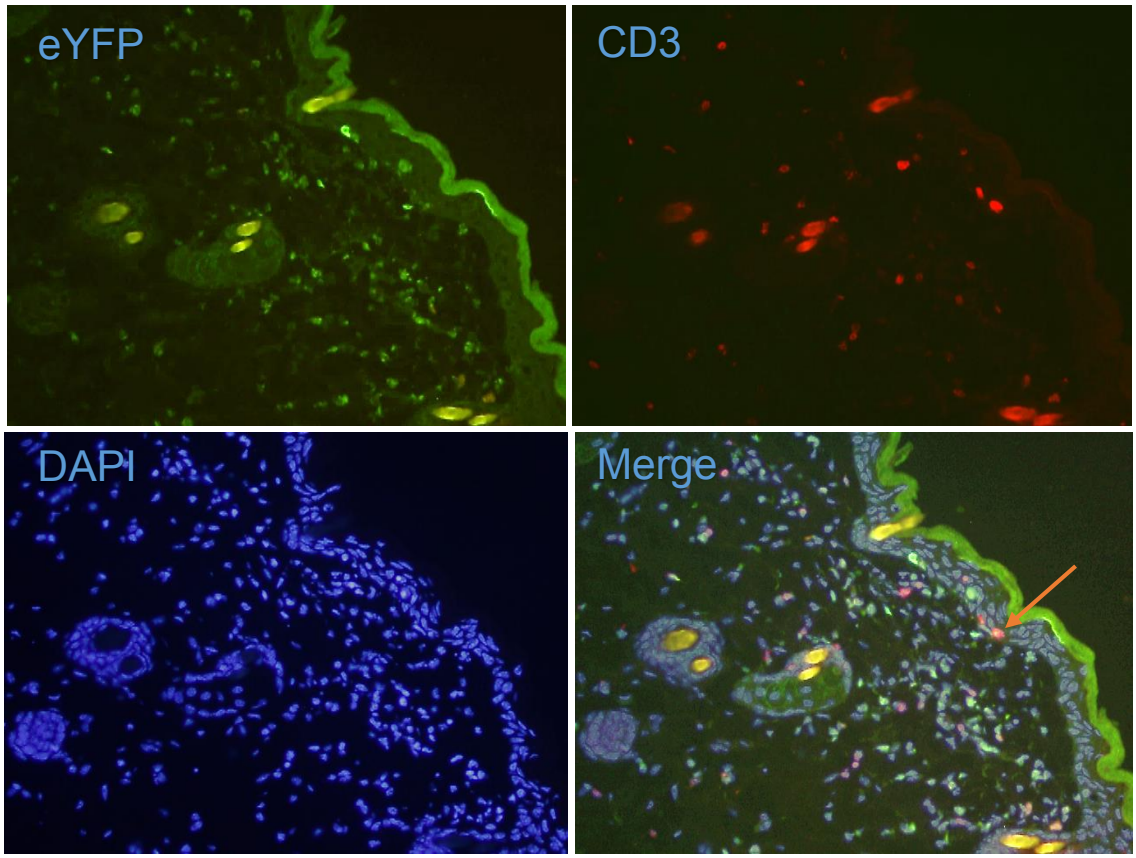

CHRY 2nd

Figure 6.2 Identification of IFNγ-producing CD3+ cells following CHRY treatment
In this study, female IFNγ reporter mice, 6 weeks old, were treated with 220 nmol chrysarobin or acetone weekly for four successive weeks. Skin was harvested at 6h following the last treatment. eYFP, CD3 and DAPI triple immunofluorescence staining were performed using 4% PFA fixed frozen sections.

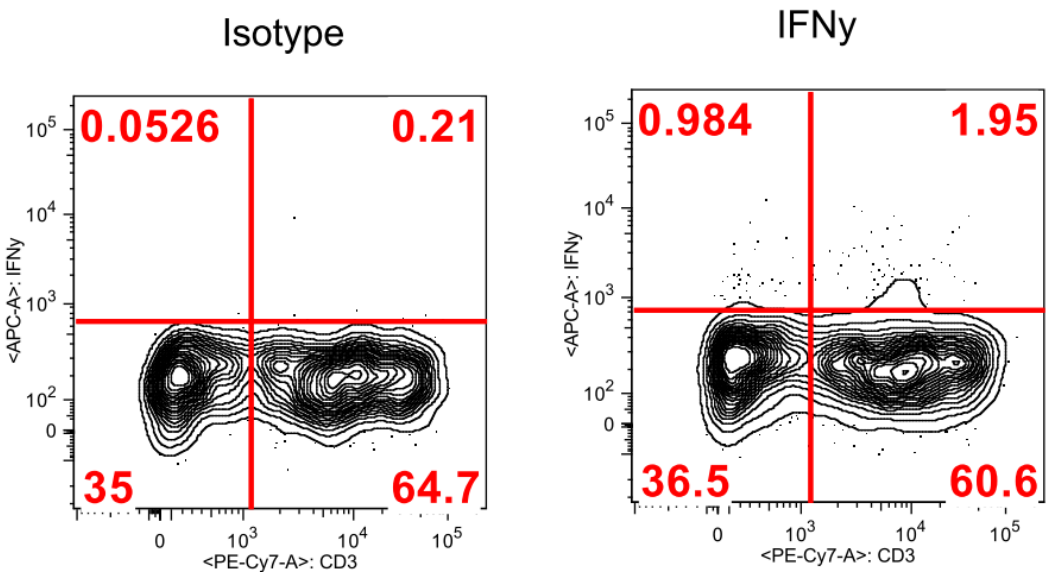

Figure 6.3 Dual fluorescence flow cytometry analysis of IFNγ-producing CD3+ cells following CHRY treatment

Six female FVB/N mice, 6-8 weeks old, were treated with 220 nmol chrysarobin weekly for four successive weeks. Skin was harvested at 4h post the last treatment. Epidermal cell suspensions were enriched for mononuclear cells (mostly lymphocyte), which were subjected to extracellular staining of PE-Cy7 conjugated CD3 antibody and intracellular staining of APC conjugated IFNγ antibody or isotype control.

Chapter 7. The Biological Impact of the SUV-induced IFNγ Signaling Activation

Mitogen-Activated Protein Kinase (MAPKs) play a major role in SUV-induced skin cancer development [94]. The pattern of SUV-induced MAPK activation has also been characterized [95]. In this study, we tested the impact of the IFNγ receptor deficiency on SUV-induced MAPK activation.

After SUV treatment on WT mice, p-p38$^{T180/Y182}$, p-JNK1/2$^{T183/Y185}$ and p-c-Jun^{S73} all increased at 6h and 24h. p-Erk1/2$^{T202/Y204}$, however, decreased after treatment (Fig 7.1). These findings are in line with the published *in vivo* data using similar treatment conditions [42]. For all these targets, IFNγR1$^{-/-}$ mice respond to SUV treatment in the same pattern, but to a lesser extent, suggesting crosstalk between SUV-induced IFNγ signaling and SUV-induced MAPKs activation.

Cxcl9, Cxcl10 and Cxcl11 are chemokines that are known to bind a common Cxcr3 receptor on both lymphoid and myeloid cells and recruit these cells to the inflammatory sites. In our study, SUV-induced IFNγ signaling activation greatly elevated the mRNA levels of Cxcl9, Cxcl10 and Cxcl11 in the skin. It was reasonable to speculate that the infiltration of immune cells caused by SUV treatment is, at least partly, dependent on the activation of IFNγ pathway and the secretion of Cxcr3 ligands. Histological analyses using a pan-myeloid marker CD11b revealed a decrease of myeloid cells influx in IFNγR1$^{-/-}$ mice compared to that in WT mice after SUV treatment (Fig. 7.2). This difference was most evident at 6h, the earliest time point examined.

There was no difference in epidermal thickness between WT and STAT1 conditional knockout mice following multiple SUV treatment. Proliferative index showed that, at 24h post last SUV treatment, WT mice had slightly higher proliferation than STAT1 conditional knockout mice (Fig 7.3). However, this difference was not statistically significant.

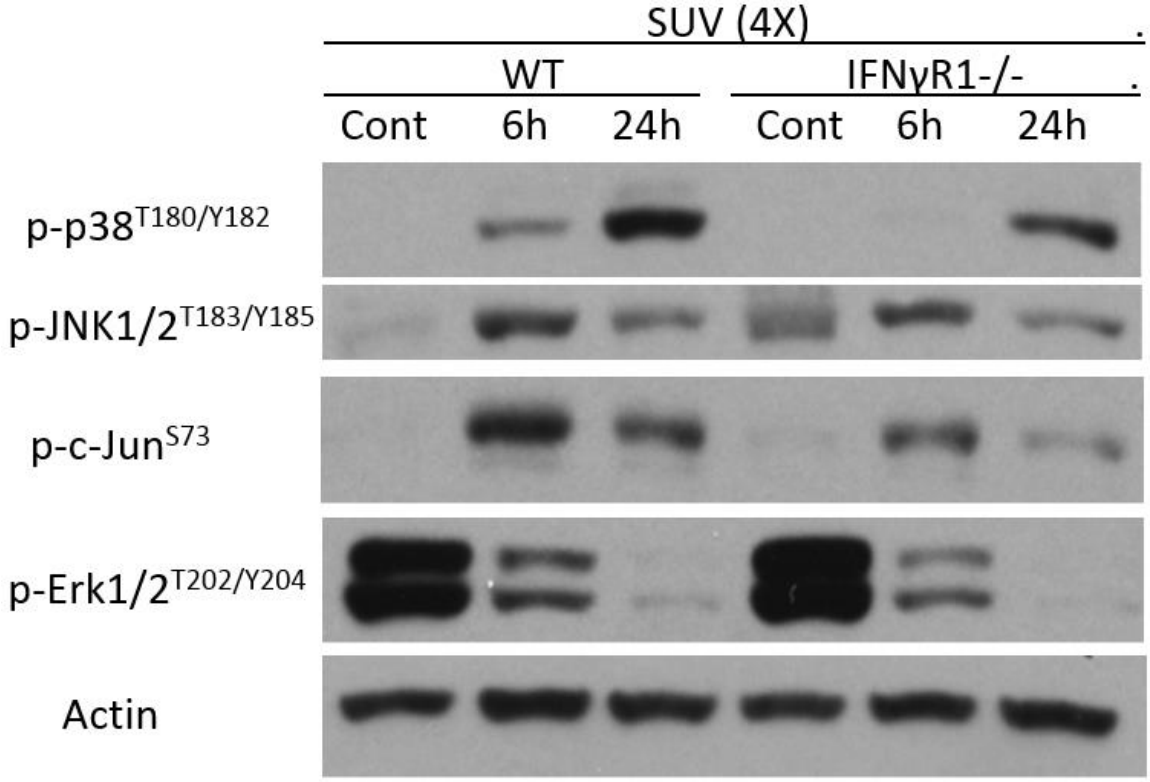

Figure 7.1 Examination of the MAPK signaling in the epidermis of IFNγR1 deficient mice with SUV treatment

Female WT and IFNγR1$^{-/-}$ mice (4/group) were treated with SUV every other day for four treatments and epidermal samples were collected at indicated time points after the last SUV treatment.

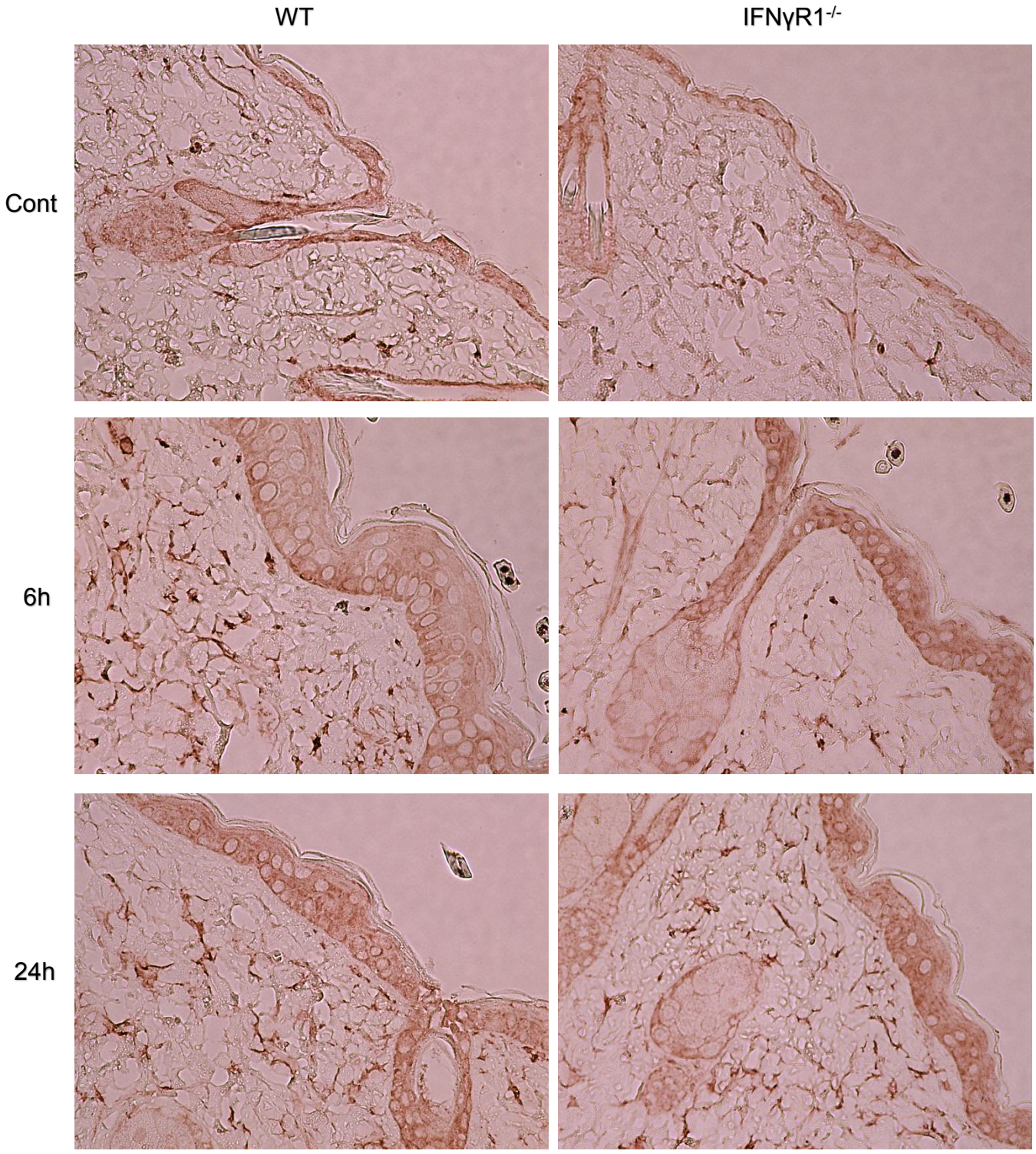

Figure 7.2 IFNγR1 deficient mice display a reduced influx of myeloid cells after SUV treatment

Female WT or IFNγR1$^{-/-}$ mice were treated with SUV every other day for four doses. Formalin-fixed paraffin-embedded skin tissues were sectioned and stained with CD11b.

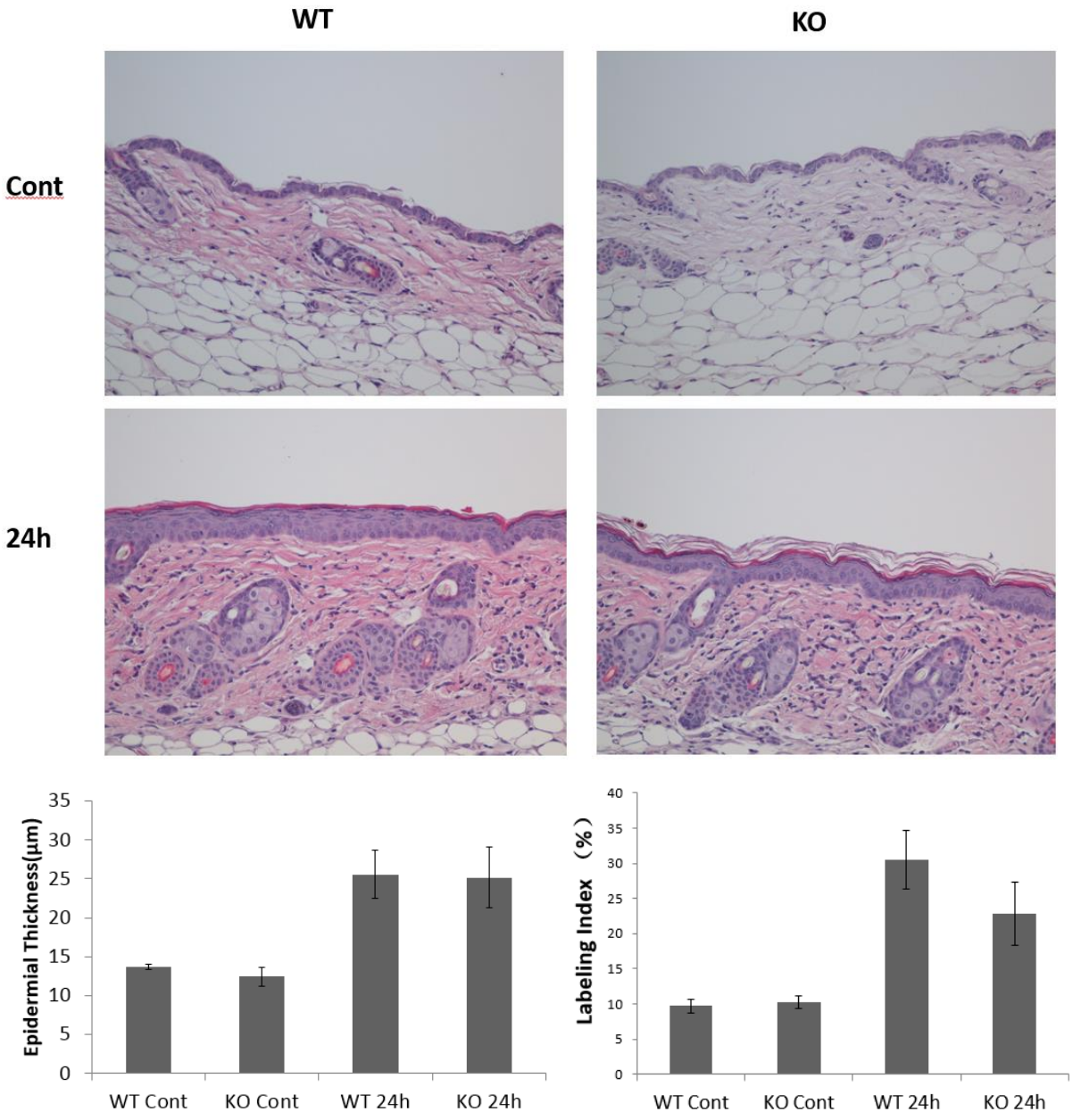

Figure 7.3 Comparisons of epidermal thickness and labeling index in WT and STAT1 skin conditional knockout mice following SUV treatment

STAT1$^{flox/flox}$ or BK5.Cre STAT1$^{flox/flox}$ mice (4/group) were treated with SUV every other day for four doses and terminated 24h following the last treatment. Formalin-fixed paraffin-embedded skin samples were sectioned for histological analyses. Epidermal thickness was measured on Hematoxylin and Eosin stained sections and labeling index was assessed by Ki67 stained sections.

Chapter 8. Discussion

In this study, we examined the possibility that SUV, a combination of UVA and UVB in a ratio close to that of sunlight, can activate the IFNγ/STAT1/IRF1 signaling axis in the epidermis of mice.

Initially, we investigated the activation pattern of IFNγ signaling pathway in mouse non-tumorigenic keratinocytes. C50 cells were treated with recombinant IFNγ in a time course experiment. IFNγ led to rapid phosphorylation of both STAT1 and STAT3 at 15 min. IRF1 and uSTAT1 proteins increased at later time points evaluated and uSTAT1 were sustained until 24h. These changes in protein levels were associated with changes in mRNA levels. Among all the downstream targets of this signaling tested, Cxcl9 and Cxcl10 mRNA showed the most substantial increase (>1000 fold). Cxcl9, Cxcl10 and Cxcl11 have a common receptor, CXCR3, which is expressed primarily on activated T lymphocytes and NK cells, and some epithelial cells. CXCR3 and its ligands form a signaling axis that has been suggested to promote skin tumorigenesis [96, 97]. Cox2 and iNOS, which are commonly associated with inflammation and cancer development, also increased at 3h post IFNγ treatment of C50 cells. PD-L1, which promotes immune evasion also increased following IFNγ stimulation. These findings together establish a well-defined pattern of how non-tumorigenic keratinocytes respond to IFNγ.

Interestingly, STAT3 was also rapidly phosphorylated in C50 cells in response to IFNγ treatment. Qing and Stark [98] suggested that Src family kinases were responsible for the phosphorylation of STAT3 in mouse embryo fibroblasts upon IFNγ treatment. However, in our experiments with C50 keratinocytes p-Src levels did not increase until 6h post IFNγ stimulation while STAT3 phosphorylation at Y705 occurred within 15 min. Incubation of C50 cells with both JAK1/2 and JAK2 inhibitors completely prevented the phosphorylation of STAT3 as well as STAT1, suggesting that JAK2, upon IFNγ stimulation, was the kinase that phosphorylates

STAT1 and STAT3. However, the importance of STAT3 phosphorylation here needs further investigation in terms of cellular response to IFNγ.

Earlier studies in our lab demonstrated that treatment with CHRY, a non-phorbol ester skin tumor promoter, led to skin tumor promotion in the two stage carcinogenesis model by a novel mechanism involving IFNγ/STAT1 signaling [82]. In the current study, utilizing IFNγ reporter mice, we further discovered that CD3+ cells in the epidermis were the main source of IFNγ production after CHRY treatment. Immunohistological analyses identified some CD3- that also contributed to IFNγ production and flow cytometry data showed that these cells represented approximately one third of the IFNγ-producing cells. These CD3- cells remain to be characterized. These data confirmed our hypothesis that CHRY treatment leads to increased production of IFNγ in immune cells resident in the epidermis.

Skin specific STAT1 deficient mice were also developed for the current study. STAT1 was knocked out in keratinocytes expressing Cre under control of the bovine keratin 5 (BK5) promoter. Similar to our previous experiments with STAT1 total body knockout mice, CHRY treatment activated IFNγ/STAT1/IRF1 signaling, which was dependent on the presence of STAT1. In keratinocyte specific STAT1 deficient mice, the increase of IRF and uSTAT1 in epidermis was substantially less than in the control group (1:3 and 1:9, respectively). This difference was not due to possible interference with IFNγ production from knocking out STAT1 as qPCR data revealed a very similar pattern of IFNγ mRNA increase at 6h post CHRY treatment in both $STAT1^{flox/flox}$ (Wildtype) and BK5.Cre.$STAT1^{flox/flox}$ mice. The detectable weak activation (Fig 4.4) could be explained by the varying efficiency of CRE-loxP system. Perhaps more significantly, other types of cells (e.g. epidermal dendritic cells) that reside in the epidermis and retain functional STAT1 in the epidermis of BK5.Cre.$STAT1^{flox/flox}$ would respond normally to IFNγ.

These data using CHRY have refined the novel mechanism of skin tumor promotion involving IFNγ/STAT1 signaling. CHRY treatment leads to the production of IFNγ in the epidermis, mostly by CD3+ cells. In the two stage carcinogenesis model, activation of IFNγ/STAT1 signaling, including rapid phosphorylation of STAT1 and subsequent induction of IRF1 and uSTAT1, in skin keratinocytes mediates the skin tumor promotion of CHRY. During the tumor promotion by CHRY, STAT1 is absolutely required as previously reported by our laboratory [82].

To bring human relevance to this novel mechanism, we tested the hypothesis that SUV activates the IFNγ/STAT1/IRF1 signaling axis in the epidermis. A time course study demonstrated an IFNγ signaling pattern very similar to what we have observed in C50 cells *in vitro* with recombinant IFNγ stimulation. In an initial experiment, qPCR data showed that IFNγ mRNA peaked at 1h following the last of four SUV treatments. In experiments using keratinocyte specific STAT1 knockout mice, we demonstrated that the induction of downstream targets including Cxcl9, Cxcl11, and IRF1 exhibited dependence on the presence of STAT1. Also, it was evident that, in IFNγR1$^{-/-}$ mice, SUV did not induce the activation of IFNγ signaling and its downstream components, suggesting that IFNγ is the primary driving force for the increase of IRF1, STAT1, Cxcl9, Cxcl10 and Cxcl11 in the epidermis after SUV treatment.

IFNγ was shown to regulate Cox2 expression in our *in vitro* experiments (Fig. 3.1) and in normal human epidermal keratinocytes [99]. The importance of Cox2 in UV-induced skin cancer has been previously validated by a number of research teams [100-102]. A variety of pathways modulate UV-induced Cox2 expression [103, 104]. However, in our experiments, both WT and IFNγR1$^{-/-}$ mice showed a dramatic increase of Cox2 mRNA following SUV treatment, indicating that IFNγ signaling was not the primary regulator of UV-induced Cox2 expression.

Given that SUV consists of UVA and UVB by the ratio of 15:1, it's intriguing to investigate the independent contribution of UVA and UVB in the induction of IFNγ signaling pathway in the epidermis. UVA is the major component of sunlight and is the major component in our SUV treatments, however on a photon-to photon basis, UVB has more energy than UVA. In a preliminary study, FVB/J mice were treated with 20 J/cm^2 UVA every other day for three treatments and there was little or no activation of IFNγ signaling (data not shown). Still, this cannot completely rule out the possibility that UVA contributed to the SUV-induced IFNγ under other treatment conditions. Merilino et al. found that IFNγ mRNA was elevated in the skin of neonatal mice following UVB treatment, which led to melanomagenesis [77]. Reeve et al., however, showed that IFNγ was involved in photoimmunoprotection by UVA radiation and that radiation with high UVA/UVB ratio upregulated the expression of cutaneous IFNγ [105, 106]. UVA irradiation, but not UVB, resulted in increased epidermal IFNγ expression peaking earlier at 1 day in hairless mice [107]. Future mechanistic study requires further analyses of untreated, UVA, UVB and SUV groups for a comprehensive comparison.

The data using IFNγ reporter mice represent the first report that CD3+ cells are the cellular source of IFNγ production upon SUV treatment. Unlike the findings of CHRY studies where some of the IFNγ producing cells in the epidermis were CD3- cells, CD3+ cells were the only cells that appeared to produce IFNγ in the epidermis following SUV treatment based on immunofluorescence. We found that the CD3+ positive cells identified in the epidermis of the control group were very abundant and displayed a profound dendritic morphology while CD3+ cells in the hyperplastic epidermis after multiple treatment were relatively sparse and did not adopt a dendritic shape. A variety of immune cells are present in normal skin, including subsets of dendritic cells and lymphocytes, as well as macrophages, mast cells and neutrophils (Fig. 8.1)[108]. There could be a significant change in

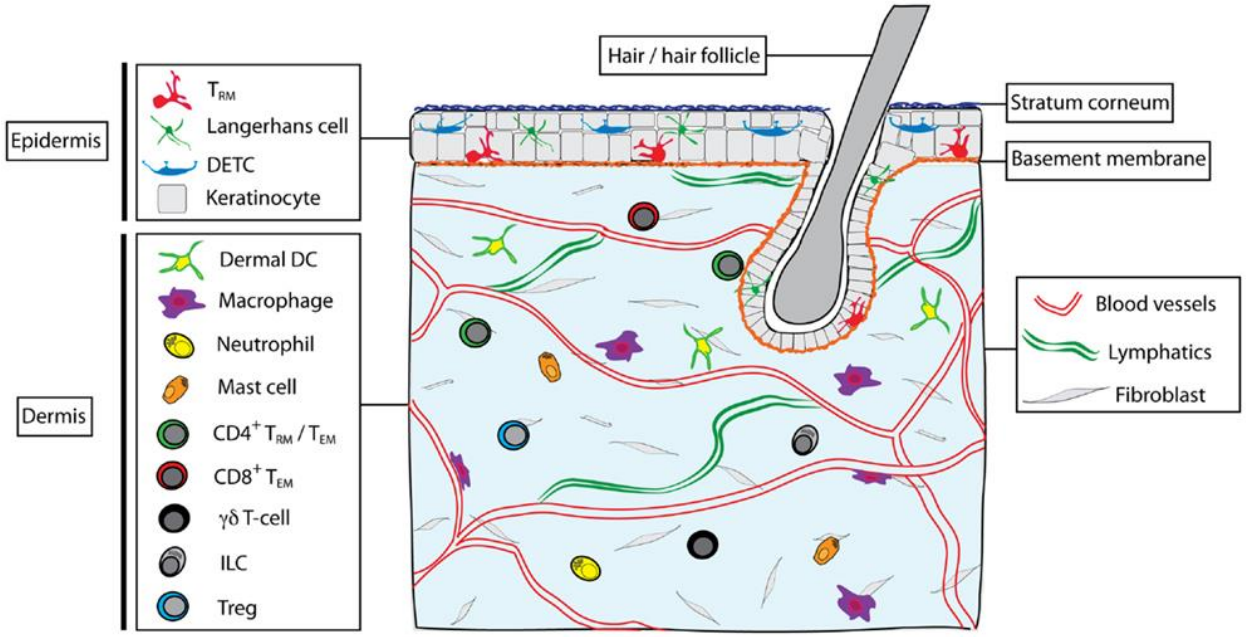

Figure 8.1 Skin structure and immune cell types found in skin

Multiple immune cells types are found within skin, including Langerhans cells, dendritic epidermal γδ T cells (DETC), and memory αβT cells (T_{RM}) in the epidermis [106].

cell types and population before and after SUV treatment, which has been reported in the literature [109]. Since CD3 is a pan T cells marker, the CD3+ cells that produced IFNγ can be further characterized. Earlier study in our lab demonstrated that single CHRY treatment caused a significant induction of IFNγ downstream targets (i.e. STAT1 and IRF1) at 6h. We believe that resident immune cells in the epidermis were responsible for the production of IFNγ because, at less than 6h post single treatment, there would not be enough time for cells in the dermis to migrate into epidermis, and then produce this cytokine. Dendritic γδ T cells have very high abundance in the epidermis and can contribute to immune response. They also form a prominent network in the skin in mice where they appear to monitor the integrity of the epidermal layer [110, 111]. In an *in vitro* experiment using an established protocol (TPA, ionomycin and Brefledin A) to stimulate IFNγ production in splenocytes, γδ T cells were competent at producing IFNγ (data not shown). Together with reports from other laboratories [112], we speculate that this CD3+ cell population can produce IFNγ following SUV treatment. Other T cells (i.e. resident memory T cells), though they reside at lower abundance in the epidermis, could also serve as the cellular source of IFNγ. Further studies will be required to distinguish these possibilities.

The biological impact of the SUV-induced IFNγ/STAT1/IRF1 signaling axis activation remains to be fully determined. The data we obtained from mice of different genetic backgrounds demonstrated a similar activation pattern at both protein level and mRNA level. We found that MAPK activation, which was reported to play a role in SUV-induced skin cancer [94], was reduced in IFNγR1$^{-/-}$ mice compared to that in WT mice. Also, after multiple SUV treatments, IFNγR1$^{-/-}$ mice displayed less myeloid cells infiltration into the dermis. Further analyses demonstrated that multiple SUV treatment led to increased epidermal thickness in both WT and STAT1 conditional knockout mice to a similar extent but WT mice has

slightly higher labeling index compared to STAT1 conditional knockout mice. This finding is similar to what we have observed in previous CHRY studies. Whether the IFNγ signaling pathway plays a role in SUV-induced skin cancer remains to be determined. Future studies are aimed at defining the role of IFNγ/STAT1 signaling axis in skin carcinogenesis by SUV.

Finally, we successfully developed a topical ointment application that inhibits STAT1 activation and transcriptional activity (i.e. STAT1 decoy; Fig 5.1). The successful formulation of this STAT1 decoy ointment provides us a useful experimental tool with substantial efficacy. The precise topical application may greatly limit the potential side effects to the whole body. One remaining issue is that mutant STAT1 decoy also had an inhibitory effect on IFNγ/STAT1 signaling pathway with a much lower efficiency compared to STAT1 decoy at the same dose. We suspect that mutant decoy still interacted with phosphorylated STAT1. A scrambled control decoy can be more suitable in future studies to eliminate any remaining affinity associated with the mutant decoy and to further define specificity.

The recurrent interaction of skin with sunlight is an intrinsic constituent of human life, and exhibits both beneficial and detrimental effects. The robust architectural framework of skin conceals remarkable mechanisms that operate at the interface between the surface and environment. The data here demonstrate that SUV induces IFNγ production from the CD3+ cells in the epidermis, and IFNγ activates IFNγ/STAT1/IRF1 signaling axis in epidermal keratinocytes, which is completely dependent on STAT1. This discovery bridges our previous finding of a novel mechanism for skin tumor promotion to solar irradiation, the major cause of human skin cancer. It also provides further avenues for future studies. The roles of IFNγ/STAT1 signaling pathway in SUV-induced skin carcinogenesis, skin disorder and pigmentation, warrant investigation in more detail.

Bibliography

1. Darnell, J.E., Jr., *STATs and gene regulation.* Science, 1997. **277**(5332): p. 1630-5.
2. Levy, D.E. and J.E. Darnell, Jr., *Stats: transcriptional control and biological impact.* Nat Rev Mol Cell Biol, 2002. **3**(9): p. 651-62.
3. Horvath, C.M., *STAT proteins and transcriptional responses to extracellular signals.* Trends Biochem Sci, 2000. **25**(10): p. 496-502.
4. Bromberg, J., *Stat proteins and oncogenesis.* J Clin Invest, 2002. **109**(9): p. 1139-42.
5. O'Shea, J.J., S.M. Holland, and L.M. Staudt, *JAKs and STATs in immunity, immunodeficiency, and cancer.* N Engl J Med, 2013. **368**(2): p. 161-70.
6. Aaronson, D.S. and C.M. Horvath, *A road map for those who don't know JAK-STAT.* Science, 2002. **296**(5573): p. 1653-5.
7. Kisseleva, T., et al., *Signaling through the JAK/STAT pathway, recent advances and future challenges.* Gene, 2002. **285**(1-2): p. 1-24.
8. O'Shea, J.J., M. Gadina, and R.D. Schreiber, *Cytokine signaling in 2002: New surprises in the JAK/Stat pathway.* Cell, 2002. **109**: p. S121-S131.
9. Rawlings, J.S., K.M. Rosler, and D.A. Harrison, *The JAK/STAT signaling pathway.* J Cell Sci, 2004. **117**(Pt 8): p. 1281-3.
10. Schindler, C., D.E. Levy, and T. Decker, *JAK-STAT signaling: from interferons to cytokines.* J Biol Chem, 2007. **282**(28): p. 20059-63.
11. McBride, K.M., et al., *Regulated nuclear import of the STAT1 transcription factor by direct binding of importin-alpha.* Embo Journal, 2002. **21**(7): p. 1754-1763.
12. Braunstein, J., et al., *STATs dimerize in the absence of phosphorylation.* Journal of Biological Chemistry, 2003. **278**(36): p. 34133-34140.
13. Ota, N., et al., *N-domain-dependent nonphosphorylated STAT4 dimers required for cytokine-driven activation.* Nature Immunology, 2004. **5**(2): p. 208-215.
14. Mao, X., et al., *Structural bases of unphosphorylated STAT1 association and receptor binding.* Molecular Cell, 2005. **17**(6): p. 761-771.
15. Zhong, M., et al., *Implications of an antiparallel dimeric structure of nonphosphorylated STAT1 for the activation-inactivation cycle.* Proc Natl Acad Sci U S A, 2005. **102**(11): p. 3966-71.
16. Mertens, C., et al., *Dephosphorylation of phosphotyrosine on STAT1 dimers requires extensive spatial reorientation of the monomers facilitated by the N-terminal domain.* Genes Dev, 2006. **20**(24): p. 3372-81.
17. Chen, X., et al., *Crystal structure of a tyrosine phosphorylated STAT-1 dimer bound to DNA.* Cell, 1998. **93**(5): p. 827-39.
18. Zhu, X., et al., *Stat1 serine phosphorylation occurs independently of tyrosine phosphorylation and requires an activated JAK2 kinase.* Mol Cell Biol, 1997. **17**(11): p. 6618-23.
19. Macias, E., D. Rao, and J. Digiovanni, *Role of stat3 in skin carcinogenesis: insights gained from relevant mouse models.* J Skin Cancer, 2013. **2013**: p. 684050.
20. Chan, K.S., et al., *Disruption of Stat3 reveals a critical role in both the initiation and the promotion stages of epithelial carcinogenesis.* J Clin Invest, 2004. **114**(5): p. 720-8.

21. Kim, D.J., et al., *Targeted disruption of stat3 reveals a major role for follicular stem cells in skin tumor initiation.* Cancer Res, 2009. **69**(19): p. 7587-94.
22. Kataoka, K., et al., *Stage-specific disruption of Stat3 demonstrates a direct requirement during both the initiation and promotion stages of mouse skin tumorigenesis.* Carcinogenesis, 2008. **29**(6): p. 1108-14.
23. Chan, K.S., et al., *Forced expression of a constitutively active form of Stat3 in mouse epidermis enhances malignant progression of skin tumors induced by two-stage carcinogenesis.* Oncogene, 2008. **27**(8): p. 1087-94.
24. Sano, S., et al., *Signal transducer and activator of transcription 3 is a key regulator of keratinocyte survival and proliferation following UV irradiation.* Cancer Res, 2005. **65**(13): p. 5720-9.
25. Kim, D.J., et al., *Signal transducer and activator of transcription 3 (Stat3) in epithelial carcinogenesis.* Mol Carcinog, 2007. **46**(8): p. 725-31.
26. Baker, S.J., S.G. Rane, and E.P. Reddy, *Hematopoietic cytokine receptor signaling.* Oncogene, 2007. **26**(47): p. 6724-37.
27. DiGiovanni, J., *Multistage carcinogenesis in mouse skin.* Pharmacol Ther, 1992. **54**(1): p. 63-128.
28. Abel, E.L., et al., *Multi-stage chemical carcinogenesis in mouse skin: fundamentals and applications.* Nat Protoc, 2009. **4**(9): p. 1350-62.
29. Rundhaug, J.E. and S.M. Fischer, *Molecular mechanisms of mouse skin tumor promotion.* Cancers (Basel), 2010. **2**(2): p. 436-82.
30. Slaga, T.J., et al., *Skin tumor-promoting activity of benzoyl peroxide, a widely used free radical-generating compound.* Science, 1981. **213**(4511): p. 1023-5.
31. DiGiovanni, J., F.H. Kruszewski, and K.J. Chenicek, *Modulation of chrysarobin skin tumor promotion.* Carcinogenesis, 1988. **9**(8): p. 1445-50.
32. Clydesdale, G.J., G.W. Dandie, and H.K. Muller, *Ultraviolet light induced injury: immunological and inflammatory effects.* Immunol Cell Biol, 2001. **79**(6): p. 547-68.
33. Chen, A.C., G.M. Halliday, and D.L. Damian, *Non-melanoma skin cancer: carcinogenesis and chemoprevention.* Pathology, 2013. **45**(3): p. 331-41.
34. Lomas, A., J. Leonardi-Bee, and F. Bath-Hextall, *A systematic review of worldwide incidence of nonmelanoma skin cancer.* British Journal of Dermatology, 2012. **166**(5): p. 1069-1080.
35. Leiter, U. and C. Garbe, *Epidemiology of melanoma and nonmelanoma skin cancer--the role of sunlight.* Adv Exp Med Biol, 2008. **624**: p. 89-103.
36. Mitra, D., et al., *An ultraviolet-radiation-independent pathway to melanoma carcinogenesis in the red hair/fair skin background.* Nature, 2012. **491**(7424): p. 449-53.
37. Hussein, M.R., *Ultraviolet radiation and skin cancer: molecular mechanisms.* J Cutan Pathol, 2005. **32**(3): p. 191-205.
38. Rodust, P.M., et al., *UV-induced squamous cell carcinoma--a role for antiapoptotic signalling pathways.* Br J Dermatol, 2009. **161 Suppl 3**: p. 107-15.
39. Bowden, G.T., *Prevention of non-melanoma skin cancer by targeting ultraviolet-B-light signalling.* Nat Rev Cancer, 2004. **4**(1): p. 23-35.
40. Scharffetter-Kochanek, K., et al., *UV-induced reactive oxygen species in photocarcinogenesis and photoaging.* Biol Chem, 1997. **378**(11): p. 1247-57.

41. Nishigori, C., Y. Hattori, and S. Toyokuni, *Role of reactive oxygen species in skin carcinogenesis.* Antioxid Redox Signal, 2004. **6**(3): p. 561-70.
42. Liu, K.D., et al., *Sunlight UV-Induced Skin Cancer Relies upon Activation of the p38 alpha Signaling Pathway.* Cancer Research, 2013. **73**(7): p. 2181-2188.
43. Oi, N., et al., *Taxifolin Suppresses UV-Induced Skin Carcinogenesis by Targeting EGFR and PI3K.* Cancer Prevention Research, 2012. **5**(9): p. 1103-1114.
44. Brennan, P., C. Fedor, and G. Pausch, *Sunlight, Uv and Accelerated Weathering.* Kunststoffe-German Plastics, 1988. **78**(4): p. 323-327.
45. Savan, R., et al., *Structural conservation of interferon gamma among vertebrates.* Cytokine & Growth Factor Reviews, 2009. **20**(2): p. 115-124.
46. Tau, G. and P. Rothman, *Review article series IV. What do knockout mice teach us about allergy? Biologic functions of the IFN-gamma receptors.* Allergy, 1999. **54**(12): p. 1233-1251.
47. Ramana, C.V., et al., *Stat1-dependent and -independent pathways in IFN-gamma-dependent signaling.* Trends Immunol, 2002. **23**(2): p. 96-101.
48. Zaidi, M.R. and G. Merlino, *The two faces of interferon-gamma in cancer.* Clin Cancer Res, 2011. **17**(19): p. 6118-24.
49. Schroder, K., et al., *Interferon-gamma: an overview of signals, mechanisms and functions.* J Leukoc Biol, 2004. **75**(2): p. 163-89.
50. Meraz, M.A., et al., *Targeted disruption of the Stat1 gene in mice reveals unexpected physiologic specificity in the JAK-STAT signaling pathway.* Cell, 1996. **84**(3): p. 431-42.
51. Durbin, J.E., et al., *Targeted disruption of the mouse Stat1 gene results in compromised innate immunity to viral disease.* Cell, 1996. **84**(3): p. 443-50.
52. Huang, S., et al., *Stat1 negatively regulates angiogenesis, tumorigenicity and metastasis of tumor cells.* Oncogene, 2002. **21**(16): p. 2504-12.
53. Lesinski, G.B., et al., *The antitumor effects of IFN-alpha are abrogated in a STAT1-deficient mouse.* J Clin Invest, 2003. **112**(2): p. 170-80.
54. Kim, H.S. and M.S. Lee, *STAT1 as a key modulator of cell death.* Cellular Signalling, 2007. **19**(3): p. 454-465.
55. Battle, T.E. and D.A. Frank, *The role of STATs in apoptosis.* Curr Mol Med, 2002. **2**(4): p. 381-92.
56. Dimco, G., et al., *STAT1 interacts directly with cyclin D1/Cdk4 and mediates cell cycle arrest.* Cell Cycle, 2010. **9**(23): p. 4638-49.
57. Huang, S.Y., et al., *Stat1 negatively regulates angiogenesis, tumorigenicity and metastasis of tumor cells.* Oncogene, 2002. **21**(16): p. 2504-2512.
58. Ursini-Siegel, J., *Beyond immune surveillance: Stat1 limits tumor growth in a cell-autonomous fashion.* Cell Cycle, 2011. **10**(9): p. 1348.
59. Koromilas, A.E. and V. Sexl, *The tumor suppressor function of STAT1 in breast cancer.* JAKSTAT, 2013. **2**(2): p. e23353.
60. Calo, V., et al., *STAT proteins: from normal control of cellular events to tumorigenesis.* J Cell Physiol, 2003. **197**(2): p. 157-68.
61. Kaplan, D.H., et al., *Demonstration of an interferon gamma-dependent tumor surveillance system in immunocompetent mice.* Proc Natl Acad Sci U S A, 1998. **95**(13): p. 7556-61.

62. Chan, S.R., et al., *STAT1-deficient mice spontaneously develop estrogen receptor alpha-positive luminal mammary carcinomas.* Breast Cancer Res, 2012. **14**(1): p. R16.
63. Adamkova, L., K. Souckova, and J. Kovarik, *Transcription protein STAT1: biology and relation to cancer.* Folia Biol (Praha), 2007. **53**(1): p. 1-6.
64. Khodarev, N.N., B. Roizman, and R.R. Weichselbaum, *Molecular pathways: interferon/stat1 pathway: role in the tumor resistance to genotoxic stress and aggressive growth.* Clin Cancer Res, 2012. **18**(11): p. 3015-21.
65. Weichselbaum, R.R., et al., *An interferon-related gene signature for DNA damage resistance is a predictive marker for chemotherapy and radiation for breast cancer.* Proc Natl Acad Sci U S A, 2008. **105**(47): p. 18490-5.
66. Magkou, C., et al., *Prognostic significance of phosphorylated STAT-1 expression in premenopausal and postmenopausal patients with invasive breast cancer.* Histopathology, 2012. **60**(7): p. 1125-32.
67. Huang, R., et al., *Increased STAT1 signaling in endocrine-resistant breast cancer.* PLoS One, 2014. **9**(4): p. e94226.
68. Hix, L.M., et al., *Tumor STAT1 Transcription Factor Activity Enhances Breast Tumor Growth and Immune Suppression Mediated by Myeloid-derived Suppressor Cells.* Journal of Biological Chemistry, 2013. **288**(17): p. 11676-11688.
69. Bailey, S.G., M.S. Cragg, and P.A. Townsend, *Role of STAT1 in the breast.* JAKSTAT, 2012. **1**(3): p. 197-9.
70. Gordziel, C., et al., *Both STAT1 and STAT3 are favourable prognostic determinants in colorectal carcinoma.* British Journal of Cancer, 2013. **109**(1): p. 138-146.
71. Kaler, P., et al., *The Role of STAT1 for Crosstalk between Fibroblasts and Colon Cancer Cells.* Front Oncol, 2014. **4**: p. 88.
72. Zhang, Y., et al., *The clinical and biological significance of STAT1 in esophageal squamous cell carcinoma.* Bmc Cancer, 2014. **14**.
73. Sanda, T., et al., *TYK2-STAT1-BCL2 pathway dependence in T-cell acute lymphoblastic leukemia.* Cancer Discov, 2013. **3**(5): p. 564-77.
74. Kovacic, B., et al., *STAT1 acts as a tumor promoter for leukemia development.* Cancer Cell, 2006. **10**(1): p. 77-87.
75. Schultz, J., et al., *Tumor-promoting role of signal transducer and activator of transcription (Stat)1 in late-stage melanoma growth.* Clinical & Experimental Metastasis, 2010. **27**(3): p. 133-140.
76. He, Y.F., et al., *Sustained low-level expression of interferon-gamma promotes tumor development: potential insights in tumor prevention and tumor immunotherapy.* Cancer Immunol Immunother, 2005. **54**(9): p. 891-7.
77. Zaidi, M.R., et al., *Interferon-gamma links ultraviolet radiation to melanomagenesis in mice.* Nature, 2011. **469**(7331): p. 548-53.
78. Cao, Y., et al., *B7-H1 overexpression regulates epithelial-mesenchymal transition and accelerates carcinogenesis in skin.* Cancer Res, 2011. **71**(4): p. 1235-43.
79. Belai, E.B., et al., *PD-1 blockage delays murine squamous cell carcinoma development.* Carcinogenesis, 2014. **35**(2): p. 424-31.
80. Furuta, J., et al., *CD271 on Melanoma Cell Is an IFN-gamma-Inducible Immunosuppressive Factor*

that Mediates Downregulation of Melanoma Antigens. Journal of Investigative Dermatology, 2014. **134**(5): p. 1369-1377.

81. Spranger, S., et al., *Up-Regulation of PD-L1, IDO, and T-regs in the Melanoma Tumor Microenvironment Is Driven by CD8(+) T Cells.* Science Translational Medicine, 2013. **5**(200).
82. Bozeman, R., et al., *A novel mechanism of skin tumor promotion involving interferon-gamma (IFNgamma)/signal transducer and activator of transcription-1 (Stat1) signaling.* Mol Carcinog, 2014.
83. Bickers, D.R. and M. Athar, *Oxidative stress in the pathogenesis of skin disease.* J Invest Dermatol, 2006. **126**(12): p. 2565-75.
84. Godic, A., et al., *The role of antioxidants in skin cancer prevention and treatment.* Oxid Med Cell Longev, 2014. **2014**: p. 860479.
85. Ichihashi, M., et al., *UV-induced skin damage.* Toxicology, 2003. **189**(1-2): p. 21-39.
86. Hennings, H., et al., *FVB/N mice: an inbred strain sensitive to the chemical induction of squamous cell carcinomas in the skin.* Carcinogenesis, 1993. **14**(11): p. 2353-8.
87. Srivastava, J., et al., *Twist1 regulates keratinocyte proliferation and skin tumor promotion.* Mol Carcinog, 2015.
88. Boehm, U., et al., *Cellular responses to interferon-gamma.* Annu Rev Immunol, 1997. **15**: p. 749-95.
89. Qing, Y. and G.R. Stark, *Alternative activation of STAT1 and STAT3 in response to interferon-gamma.* J Biol Chem, 2004. **279**(40): p. 41679-85.
90. Mann, M.J. and V.J. Dzau, *Therapeutic applications of transcription factor decoy oligonucleotides.* J Clin Invest, 2000. **106**(9): p. 1071-5.
91. Wan, J., et al., *Oligonucleotide therapeutics in cancer.* Cancer Treat Res, 2013. **158**: p. 213-33.
92. Dean, N.M. and C.F. Bennett, *Antisense oligonucleotide-based therapeutics for cancer.* Oncogene, 2003. **22**(56): p. 9087-96.
93. Ruscher, K., et al., *Erythropoietin is a paracrine mediator of ischemic tolerance in the brain: Evidence from an in vitro model.* Journal of Neuroscience, 2002. **22**(23): p. 10291-10301.
94. Bode, A.M. and Z. Dong, *Mitogen-activated protein kinase activation in UV-induced signal transduction.* Sci STKE, 2003. **2003**(167): p. RE2.
95. Schieke, S.M., et al., *Molecular crosstalk of the ultraviolet a and ultraviolet B signaling responses at the level of mitogen-activated protein kinases.* J Invest Dermatol, 2005. **124**(4): p. 857-9.
96. Winkler, A.E., et al., *CXCR3 Enhances a T-Cell-Dependent Epidermal Proliferative Response and Promotes Skin Tumorigenesis.* Cancer Research, 2011. **71**(17): p. 5707-5716.
97. Gorbachev, A., D. Kish, and R. Fairchild, *Modulating CXCR3 chemokine expression in the tumor microenvironment as a therapeutic approach for skin cancers.* Journal of Immunology, 2013. **190**.
98. Qing, Y.L. and G.R. Stark, *Alternative activation of STAT1 and STAT3 in response to interferon-gamma.* Journal of Biological Chemistry, 2004. **279**(40): p. 41679-41685.
99. Matsuura, H., et al., *Regulation of cyclooxygenase-2 by interferon gamma and transforming growth factor alpha in normal human epidermal keratinocytes and squamous carcinoma cells. Role of mitogen-activated protein kinases.* J Biol Chem, 1999. **274**(41): p. 29138-48.
100. Fischer, S.M., et al., *Cyclooxygenase-2 expression is critical for chronic UV-induced murine skin carcinogenesis.* Mol Carcinog, 2007. **46**(5): p. 363-71.

101. Rundhaug, J.E., et al., *A role for cyclooxygenase-2 in ultraviolet light-induced skin carcinogenesis.* Mol Carcinog, 2007. **46**(8): p. 692-8.
102. Tripp, C.S., et al., *Epidermal COX-2 induction following ultraviolet irradiation: suggested mechanism for the role of COX-2 inhibition in photoprotection.* J Invest Dermatol, 2003. **121**(4): p. 853-61.
103. Tang, Q., et al., *Roles of Akt and glycogen synthase kinase 3beta in the ultraviolet B induction of cyclooxygenase-2 transcription in human keratinocytes.* Cancer Res, 2001. **61**(11): p. 4329-32.
104. Chen, W., et al., *Role of p38 MAP kinases and ERK in mediating ultraviolet-B induced cyclooxygenase-2 gene expression in human keratinocytes.* Oncogene, 2001. **20**(29): p. 3921-6.
105. Reeve, V.E., M. Bosnic, and N. Nishimura, *Interferon-gamma is involved in photoimmunoprotection by UVA (320-400 nm) radiation in mice.* Journal of Investigative Dermatology, 1999. **112**(6): p. 945-950.
106. Reeve, V.E., D. Domanski, and M. Slater, *Radiation sources providing increased UVA/UVB ratios induce photoprotection dependent on the UVA dose in hairless mice.* Photochem Photobiol, 2006. **82**(2): p. 406-11.
107. Shen, J., S. Bao, and V.E. Reeve, *Modulation of IL-10, IL-12, and IFN-gamma in the epidermis of hairless mice by UVA (320-400 nm) and UVB (280-320 nm) radiation.* J Invest Dermatol, 1999. **113**(6): p. 1059-64.
108. Mueller, S.N., A. Zaid, and F.R. Carbone, *Tissue-resident T cells: dynamic players in skin immunity.* Front Immunol, 2014. **5**: p. 332.
109. Sluyter, R. and G.M. Halliday, *Enhanced tumor growth in UV-irradiated skin is associated with an influx of inflammatory cells into the epidermis.* Carcinogenesis, 2000. **21**(10): p. 1801-7.
110. Chodaczek, G., et al., *Body-barrier surveillance by epidermal gamma delta TCRs.* Nature Immunology, 2012. **13**(3): p. 272-U96.
111. Vantourout, P. and A. Hayday, *Six-of-the-best: unique contributions of gamma delta T cells to immunology.* Nature Reviews Immunology, 2013. **13**(2): p. 88-100.
112. Gao, Y., et al., *Gamma delta T cells provide an early source of interferon gamma in tumor immunity.* J Exp Med, 2003. **198**(3): p. 433-42.

Vita

Tianyi Cheng was born in 1989 in Hefei, China where he lived with his parents. After completed his work at Hefei No.1 High School in 2007, he entered China Pharmaceutical University in Nanjing, China and he received the Bachelor degree of Engineering in Biotechnology in June, 2011. During the spring of 2011, he attended Rutgers University, NJ, USA in an exchange program. In September, 2012, he entered the University of Texas at Austin, College of Pharmacy to start his graduate studies under the guidance of Dr. John DiGiovanni.

Address: c.tianyi1989@gmail.com

This manuscript was typed by the author.